https://doi.org/10.5194/acp-2019-493
Preprint. Discussion started: 18 June 2019
© Author(s) 2019. CC BY 4.0 License.

Atmospheric Chemistry and Physics Discussions

Long range and local air pollution: what can we learn from chemical speciation of particulate matter at paired sites?

Marco Pandolfi [a,*], Dennis Mooibroek [b], Philip Hopke [c], Dominik van Pinxteren [d], Xavier Querol [a], Hartmut Herrmann [d], Andrés Alastuey [a], Olivier Favez [e], Christoph Hüglin [f], Esperanza Perdrix [g], Véronique Riffault [g], Stéphane Sauvage [g], Eric van der Swaluw [b], Oksana Tarasova [h], and Augustin Colette [e]

[a] Institute of Environmental Analysis and Water Research (IDAEA-CSIC), c/ Jordi-Girona 18-26, Barcelona, Spain
[b] Centre for Environmental Monitoring, National Institute of Public Health and the Environment (RIVM), A. van Leeuwenhoeklaan 9, P.O. Box 1, 3720 BA, Bilthoven, The Netherlands
[c] Center for Air Resources Engineering and Science, Clarkson University, Potsdam, NY, USA
[d] Leibniz Institute for Tropospheric Research (TROPOS), Atmospheric Chemistry Department (ACD), Permoserstr. 15, 04318 Leipzig, Germany
[e] National Institute for Industrial Environment and Risks (INERIS), Verneuil-en-Halatte, 60550, France
[f] Empa, Swiss Federal Laboratories for Materials Science and Technology, 8600 Dübendorf, Switzerland
[g] IMT Lille Douai, Univ. Lille, SAGE – Département Sciences de l'Atmosphère et Génie de l'Environnement, 59000 Lille, France
[h] World Meteorological Organization, Research Department, Geneva, Switzerland

* Corresponding author: Marco Pandolfi (marco.pandolfi@idaea.csic.es)

Abstract

We report here results of a detailed analysis of the urban and non-urban contributions to PM concentrations and source contributions in 5 European cities, namely: Shiedam (The Netherlands; NL), Lens (France; FR), Leipzig (Germany; DE), Zurich (Switzerland; CH) and Barcelona (Spain; ES). PM chemically speciated data from 12 European paired monitoring sites (1 traffic, 5 urban, 5 regional and 1 continental background) were analyzed by Positive Matrix Factorization (PMF) and Lenschow's approach to assign measured PM and source contributions to the different spatial levels. Five common sources were obtained at the 12 sites: *sulfate-rich* (SSA) and *nitrate-rich* (NSA) aerosols, *road traffic* (RT), *mineral matter* (MM), and *sea salt* (SS). These sources explained from 55% to 88% of PM mass at urban low-traffic impact

https://doi.org/10.5194/acp-2019-493
Preprint. Discussion started: 18 June 2019
© Author(s) 2019. CC BY 4.0 License.

Atmospheric Chemistry and Physics Discussions

sites (UB) depending on the country. Three additional common sources were detected at a subset of sites/countries, namely: *biomass burning* (BB) (FR, CH, and DE), explaining an additional 9-13% of PM mass, *residual oil combustion* (V-Ni), and *primary industrial* (IND) (NL and ES), together explaining an additional 11-15% of PM mass. In all countries, the majority of PM measured at UB sites was of regional+continental (R+C) nature (64-74%). The R+C PM increments due to anthropogenic emissions were in the range 10-11 $\mu g/m^3$ in CH, NL and DE (52%, 62% and 66%, respectively, of UB PM mass), followed by ES (8 $\mu g/m^3$; 32%) and FR (5 $\mu g/m^3$; 23%). Overall, the R+C PM increments due to natural and anthropogenic sources showed opposite seasonal profiles with the former increasing in summer and the latter increasing in winter, even if exceptions were observed. In ES, the anthropogenic R+C PM increment was higher in summer due to high contributions from regional SSA and V-Ni sources, both being mostly related to maritime shipping emissions at the Spanish sites. Conversely, in the other countries, higher anthropogenic R+C PM increments in winter were mostly due to high contributions from NSA and BB regional sources during the cold season. On annual average, the sources showing higher R+C increments were SSA (77-91% of SSA source contribution at urban level), NSA (51-94%), MM (58-80%), BB (42-78%), IND (91% in the Netherlands). Other sources showing high R+C increments were photochemistry (PHO) and coal combustion (CC) (97-99%; detected only in DE). The highest regional SSA increment was observed in ES, especially in summer, and was related to ship emissions, enhanced photochemistry and peculiar meteorological patterns of the Western Mediterranean. The highest R+C and urban NSA increments were observed in NL and associated with high availability of precursors such as NO_x and NH_3. Conversely, on average, the sources showing higher local increments were RT (62-90% at all sites) and V-Ni (65-80% in ES and NL). The relationship between SSA and V-Ni indicated that the contribution of ship emissions to the local sulfate concentrations in NL strongly decreased from 2007 thanks to the shift from high-sulfur to low-sulfur content fuel used by ships. Based on the present analysis, an improvement of air quality in the 5 cities included here could be achieved by further reducing local (urban) emissions of PM, NO_x and NH_3 (from both traffic and non-traffic sources) but also SO_2 and PM (from maritime ships and ports) and giving high relevance to non-urban contributions by further reducing emissions of SO_2 (maritime shipping) and NH_3 (agriculture) and those from industry, regional BB sources and coal combustion.

https://doi.org/10.5194/acp-2019-493
Preprint. Discussion started: 18 June 2019
© Author(s) 2019. CC BY 4.0 License.

Atmospheric Chemistry and Physics Discussions

1. Introduction

In the last scientific assessment report from the Convention on Long-Range Transboundary Air Pollution (CLRTAP) “Toward Cleaner Air”, it is stated that because non-urban sources (i.e. regional+continental sources) are often major contributors to urban pollution, many cities will be unable to meet WHO guideline levels for air pollutants through local action alone. Consequently, it is very important to estimate how much the local and regional+continental (R+C) sources (both natural and anthropogenic) contribute to urban pollution in order to design global strategies to reduce the levels of pollutants in European cities.

There are various modelling approaches to disentangle the local/remote contribution to urban air pollution. But it is also relevant to investigate how in-situ measurements can be used for that purposed. The Task Force on Measurements and Modeling (TFMM-CLRTAP) therefore initiated an assessment of the added value of paired urban and regional/remote sites in Europe. Experimental data from paired sites were used to allocate urban pollution to the different spatial scale sources. The paired sites selected for this study provided chemically speciated PM_{10} or $PM_{2.5}$ data simultaneously measured at urban/traffic and regional/remote sites. In some cases, (e.g. Spain; ES) these measurements were continuously performed over long periods, whereas in other cases the measurements were performed for a limited time period. The periods presented here were comparable in Switzerland (CH; 2008-2009) and the Netherlands (NL; 2007-2008), whereas more recent data were used for Spain (ES; 2010 – 2014), Germany (DE; 2013-2014) and France (FR; 2013 – 2014).

The approach proposed and described in this paper aimed at identifying the urban and non urban (R+C) contributions (or a mix of both) to the PM mass measured at urban level and at calculating the urban increments that corresponds to the concentration difference between the city and the regional locations.

Moreover, we were able to allocate urban and non-urban pollution to major primary sources by activity sector or to main secondary aerosol fractions thanks to the application of Positive Matrix Factorization (PMF) (described below) that quantitatively groups species emitted from the same source. This information is useful for devising opportune abatement/mitigation strategies to tackle air pollution.

Chemistry Transport Models (CTMs) are regularly used to design air pollution mitigation strategies and a recurring question regards the identification of the main activity sectors and geographical areas that produce the pollutants. The performances of CTMs in this identification must therefore be compared to measurements. A first step consists in comparing the chemical composition of PM between models and

https://doi.org/10.5194/acp-2019-493
Preprint. Discussion started: 18 June 2019
© Author(s) 2019. CC BY 4.0 License.

Atmospheric Chemistry and Physics Discussions

observations. Such comparison has been performed before for specific areas or overall for Europe (Bessagnet et al., 2016), but the synthesis presented in the present paper will be particularly relevant to identify the main characteristics of the diversity of sites in terms of both chemical composition and urban/regional gradients. In a second step, a comparison with the models that provide a direct quantification of activity sectors is also relevant. Whereas CTMs focus essentially on chemical composition, some models (e.g. the TNO LOTOS-EURO; Kranenburg et al., 2013) include a tagging or source apportionment information (also referred to as source oriented models). However, we can also include Integrated Assessment Models such as GAINS (Amann et al., 2011; Kiesewetter et al., 2015) or SHERPA (Pisoni et al., 2017) or even the Copernicus Atmosphere Monitoring Service (CAMS) Policy Service (http://policy.atmosphere.copernicus.eu). In various ways, these tools propose a quantification of the priority activity sectors and scale for actions that must be targeted when designing air quality policies, although these models are challenging to compare with observations.

2. Methodology

The proposed methodology consists in the application of Lenschow's approach (Lenschow et al., 2001) to the source contributions calculated by means of PMF at appropriately paired sites to assess the increments of air pollution.

2.1 PMF model

PMF (EPA PMFv5.0) was applied to the collected daily PM speciated data for source identification and apportionment. PMF was applied to the PM chemically speciated data from ES, CH, and FR. For NL and DE, we used the PMF analysis already presented in Mooibroek et al. (2011) and van Pinxteren et al. (2016), respectively, and then applying the Lenschow approach to the PMF outputs.

Detailed information about PMF can be found in the literature (e.g. Paatero and Tapper, 1994; Paatero, 1999; Paatero and Hopke, 2003; Paatero and Hopke, 2008; Hopke, 2016). PMF is a factor analytical tool that reduces the dimension of the input matrix (i.e. the daily chemically speciated data) to a limited number of factors (or sources). It is based on the weighted least squares method and uses the uncertainties of the input data to solve the chemical mass balance equations. In the present study, individual uncertainties and detection limits were calculated in different ways, depending on the available information about analytical uncertainties.

https://doi.org/10.5194/acp-2019-493
Preprint. Discussion started: 18 June 2019
© Author(s) 2019. CC BY 4.0 License.

Atmospheric Chemistry and Physics Discussions

One approach (applied to the Spanish database) was based on the use of both the analytical uncertainties and the standard deviations of species concentrations in the blank filters for uncertainties calculations. This approach was described in Escrig et al. (2009) and Amato et al. (2009). For the French sites, the uncertainty calculations for the trace elements was performed using the expanded relative uncertainties for each species and the total uncertainties were calculated by multiplying these relative uncertainties by the concentration of each species (Waked et al., 2014 and references herein). These relative uncertainties included variability from contamination, sampling volume, repeatability and accuracy (through the digestion recovery rate determinations). Finally, an expanded relative uncertainty of 10% was used for OC, 15% for EC, and 15% for monosaccharide sugars such as levoglucosan, arabitol, sorbitol, and mannitol. For the Swiss and Dutch sites, the uncertainties were estimated using information about the minimum detection limit (MDL) of the techniques used for chemical analysis. In this approach, data below the MDL were replaced by half the MDL and the corresponding uncertainty was set to 5/6 times the MDL (Polissar et al., 1998; Kim et al., 2003; Kim and Hopke, 2008). For the German sites, the uncertainty matrix was constructed from 3 components: (i) uncertainty of the instrumental limit of detection (LOD), defined as 5/6 of the LOD, (ii) analytical uncertainty, obtained from relative standard deviations of signal intensities from repeated standard measurements, and (iii) uncertainty of the mean field blank concentration, defined as 3 times the standard deviation of the field blank. Total uncertainty was calculated from these components applying Gaussian error propagation (details in van Pinxteren et al., 2016).

The signal-to-noise ratio (S/N) was estimated starting from the calculated uncertainties and used as a criterion for selecting the species used within the PMF model. In order to avoid any bias in the PMF results, the data matrix was uncensored (Paatero, 2004). The PMF was run in robust mode (Paatero, 1997). The optimal number of sources was selected by inspecting the variation of the objective function Q (defined as the ratio between residuals and errors in each data value) with a varying number of sources (i.e., Paatero et al., 2002) and by studying the distribution of the scaled residuals for each variable.

2.1.1 Multi-site PMF

In this work, we used the chemically speciated data from 24h samples collected at the paired sites available in a country combining together the datasets from the available site pairs (multi-site PMF) as the PMF input. Thus, the hypothesis is that the chemical

https://doi.org/10.5194/acp-2019-493
Preprint. Discussion started: 18 June 2019
© Author(s) 2019. CC BY 4.0 License.

Atmospheric Chemistry and Physics Discussions

profiles of the sources are similar at the paired sites. If this hypothesis is not satisfied, then the multi-site PMF could lead to undesired uncertainties in the estimation of the source contributions. In the following sections, we demonstrate the feasibility of the multi-site PMF for each country. However, it is important to consider that we can only apply the Lenschow approach to exactly the same variables (same pollutant sources in this case) that can be only obtained through the application of the multi-site PMF.

To demonstrate the feasibility of the multi-site PMF, we compared the source profiles from the multi-site PMF with the source profiles from the individual single-site PMF results (Sofowote et al., 2015). This procedure was applied to the PMF outputs obtained for ES, FR, and CH. For NL and DE, as stated before, the multi-site PMF was already published. Thus, we did not perform the sensitivity study for Dutch and German databases.

The feasibility of the multi-site PMF depends on the degree of similarity of the source profiles among the PMF runs. For the comparison, we calculated the ratio between specific tracers in each chemical profile for each PMF run and then we calculated the coefficient of variation (CV) of the obtained ratios. As an example, for the *sulfate-rich* source we compared the $[NH_4^+]/[SO_4^{2-}]$ ratios. Sofowote et al. (2015) suggested that if CV of the ratios for each chemical profile is lower than 20-25%, multi-site PMF is applicable. If this condition is satisfied, we can assume that the chemical profiles of the obtained sources are similar at the paired sites. For this sensitivity test, the number and types of sources from each PMF run (single and multi-site) should be the same.

The robustness of the detected sources in each PMF run can be estimated using some of the tools available in the EPA PMF version 5.0 such as the bootstrapping resampling and the displacement of factor elements or both (Paatero et al., 2014; Brown et al., 2015).

The main advantage of the multi-site PMF is that a larger dataset is used in the PMF model compared to the separate single-site PMFs. Thus, multi-site PMF is more likely to include low contribution (edge point) values and produce more robust results. Moreover, by combining the datasets, the analysis will provide insight into the sources affecting both receptor sites, and will most likely tend to focus on the general phenomena instead of the unique local variations (Escrig et al., 2009).

Additionally, pooling the concentrations of PM constituents collected at the paired sites into one dataset allows the application of the Lenschow's approach detailed below. To obtain the net local source impacts, the source contributions estimated at the regional station are subtracted from the source contributions estimated at the urban

https://doi.org/10.5194/acp-2019-493
Preprint. Discussion started: 18 June 2019
© Author(s) 2019. CC BY 4.0 License.

Atmospheric Chemistry and Physics Discussions

station. Thus, we need that the sources detected at the paired sites are exactly the same and for this reason, multi-site PMF was performed.

2.2 The Lenschow's approach

Lenschow's approach (Lenschow et al., 2001) is a simple technique that aims at assessing the contribution of pollutants from different spatial scales (i.e. local, regional, continental) into the urban concentration.

Depending on the country, different paired sites were available for this analysis (traffic/urban/regional/remote). The descriptions of the sites are given in the next section. Lenschow's approach implies some important assumptions to assess the increments at various sites in terms of actual contributions:

- The differences of source contributions between a traffic station (TS) and a urban low-traffic impact sites (UB) station can be attributed to the very local influence of traffic (and other very local sources) on the adjacent street/district. This difference is called *traffic increment*.
- The differences between an UB station and a rural background (RB) station can be attributed to the sources of the agglomeration such as building heating or the dispersed traffic increment. This difference is called *urban increment*.

If a remote (i.e. mountain top station/continental background station (CB)) is also available, then we assume that:

- The differences of the source contributions between the RB and CB stations can be attributed to the regional sources with little contribution from the urban agglomeration. This difference is called *regional increment*.
- The source contributions at the CB station can be attributed to continental sources. This contribution is called *continental increment*.

If only the RB station is available we cannot separate the regional and continental contributions, therefore we assume that:

- The source contributions at the RB station can be attributed to both regional and continental sources (without the possibility to separate the two contributions) with little contribution from the urban agglomeration.

The important hypothesis behind Lenschow's approach is that the emissions from the city should not directly affect the regional/remote site, otherwise this approach

https://doi.org/10.5194/acp-2019-493
Preprint. Discussion started: 18 June 2019
© Author(s) 2019. CC BY 4.0 License.

Atmospheric Chemistry and Physics Discussions

will lead to an underestimation of the urban increment. The city contribution to the measured RB levels (called "city spread" in Thunis et al., 2018) also depends on the distance between the city and the RB station. The larger the distance between the UB and RB sites, the lower should be the city impacts. Moreover, as suggested by Thunis et al. (2018), the size of the city is also a parameter that can affect the city effect. Another consideration is that: a) specific meteorological conditions favoring the transport of the city emissions to the RB site can also contribute to the city spread, and b) even if the city emissions do not influence the RB site, nearby rural emissions might increase RB levels of PM. This issue is made even more complex when considering the different lifetime of chemical species. Whereas the dispersion of primary species will be primarily constrained by the geometry of the sources, the topography of the areas and the meteorological dispersion patterns, for secondary species, the chemical formation process introduces a substantial complexity.

2.3 Paired sites and measurements

In the following, we provide a brief description of the paired sites included in this analysis and the PM chemically speciated data available in each country. Figure 1 shows the location of the paired sites, whereas the main statistics of the chemical species used in the PMF model is provided in Tables S1-S4.

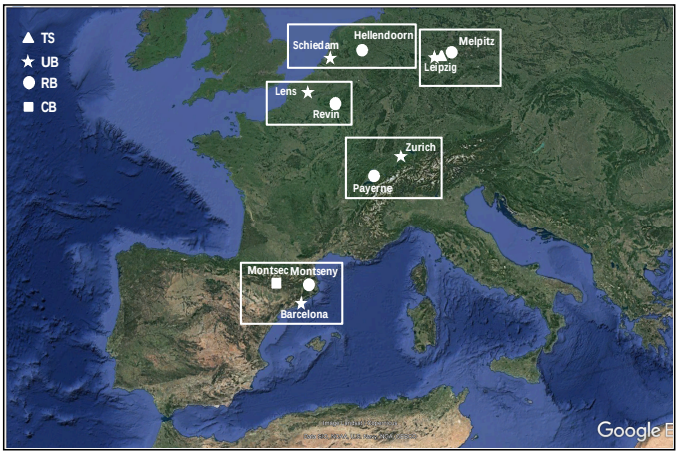

Figure 1: Paired sites included in this work. TS: Traffic station (DE). UB: Urban background (NL, DE, FR, CH, ES); RB: Regional background (NL, DE, FR, CH, ES); CB: Continental background (ES);

https://doi.org/10.5194/acp-2019-493
Preprint. Discussion started: 18 June 2019
© Author(s) 2019. CC BY 4.0 License.

Atmospheric Chemistry and Physics Discussions

- *Spain (ES)*

Three sites were available in ES, namely: the *Barcelona* UB station (BCN; 41°23'24.01'' N, 02°6'58.06'' E, 64 m a.s.l.), the *Montseny* RB station (MSY; 41°46'45.63'' N, 02°21'28.92'' E, 720 m a.s.l.) and the *Montsec* CB (MSA; 42°3' N, 0°44' E, 1570 m a.s.l.). These stations are run by the EGAR Group of the Institute of Environmental Assessment and Water Research (IDAEA-CSIC) in Barcelona. The BCN site is an urban background measurement site influenced by vehicular emissions from one of the main avenues of the city (Diagonal Avenue) located at a distance of around 300 m. Several industrial zones, power plants, and highways are located in the Metropolitan area of Barcelona, making this region one of the most polluted in the Western Mediterranean Basin (i.e., Querol et al., 2008; Amato et al., 2009; Pandolfi et al., 2014). The MSY site is a RB site in the NE of Spain, located in a regional natural park about 50 km to the NNE of the city of Barcelona (BCN) and 25 km from the Mediterranean coast. This site is representative of the typical regional background conditions of the Western Mediterranean Basin (i.e., Pérez et al., 2008; Pey et al., 2010; Pandolfi et al., 2011, 2014). This station is part of the ACTRIS (Aerosol, Clouds, and Trace gases Research Infrastructure, www.actris.net) and GAW (Global Atmosphere Watch Programme, www.wmo.int/gaw) networks and of the measuring network of the government of Catalonia. The MSA site (also part of ACTRIS and GAW networks) is a CB high altitude observatory located in the NE of the Iberian Peninsula and situated in the southern side of the Pre-Pyrenees at the top of Montsec d'Ares (e.g. Ripoll et al., 2014; Pandolfi et al., 2014a). This region has a low density population and is isolated from large pollutant emissions, 140 km from the BCN to the southeast, 30 km from the largest city in the region (Balaguer, 15 769 inhabitants) to the south, and 50 km from the axial Pyrenees to the north.

Measurements of PM_{10} chemically speciated data from the three Spanish sites used here covered the period 2010 – 2014. Details on the analytical methods used can be found for example in Querol et al. (2007) and Pandolfi et al. (2016). A total of 2115 samples were used in the PMF model. Table S1 in Supporting Materials reports the chemical species included in PMF analysis and the main statistics (mean, median, SD) for each species for the three Spanish sites.

- *Switzerland (CH)*

Two measuring sites were available in CH: a UB station in Zurich (*Zurich-Kaserne,* ZUE; 47°22'36.42'' N, 8°31'44.70'' E, 410 m a.s.l.) and the RB station of Payerne (PAY; 46°49'12'' N, 06°57' E, 491 m a.s.l.). ZUE station has been characterized in previous

https://doi.org/10.5194/acp-2019-493
Preprint. Discussion started: 18 June 2019
© Author(s) 2019. CC BY 4.0 License.

Atmospheric Chemistry and Physics Discussions

studies (Gehrig and Buchmann, 2003; Hueglin et al., 2005; Szidat et al., 2006; Bukowiecki et al., 2010; Lanz et al., 2008). It is a courtyard shielded from direct emissions by its surrounding walls. In addition, the roads in its vicinity belong to residential areas with only minor traffic density. The site is part of the Swiss National Air Pollution Monitoring Network (NABEL). PAY is a RB air quality monitoring station located in Southwestern Switzerland in the basin between the Jura and the Alps. It is about 1 km south-east of the small rural town of Payerne. The site is surrounded by agricultural land (grassland and crops), forests, and small villages. The station is part of the EMEP and GAW networks. The distance between ZUE and PAY is more than 130 km.

Measurements of PM_{10} chemically speciated data were available at the two sites during the period August 2008 – July 2009 (Gianini et al., 2012). A total of 178 samples (89 collected at ZUE and 89 collected at PAY) and 31 species (listed in Table S2) were used in the PMF analysis. Table S2 reports the summary statistics for these chemical species .

- The Netherlands (NL)

The measuring sites and the $PM_{2.5}$ chemically speciated data available in NL were presented by Mooibroek et al. (2011) where data from 5 stations (one TS, one UB and three RB sites) were simultaneously used in the PMF model in order to document the variability of the $PM_{2.5}$ source contributions in NL. Here, we used data from two stations (Schiedam (SCH; UB) and Hellendoorn (HEL; RB)) and removing from the analysis the TS site (Rotterdam) and two RB sites (Vredepeel and Cabauw). The Rotterdam TS site was excluded because the calculated TS increments from Lenschow's approach (Rotterdam minus SCH) were negative for many of the sources calculated for NL (*Mineral, Sea Spray, Residual Oil and sulfate-rich*). The Cabauw RB site was excluded because it is surrounded by urban agglomerations leading to an increased contributions of traffic from those nearby urbanized areas. Therefore, the traffic contribution at the urban location could be underestimated if Cabauw was used. The other RB station (Vredepeel) was removed mainly because it is influenced by agricultural activities in that area. Below a brief description of the two sites used here: SCH (51°55'1.43"N, 4°23'55.16" E) is an UB site located in the west of NL. It is part of Rotterdam agglomeration. Rotterdam has approximately 600,000 inhabitants close to refineries and harbor related activities (Port of Rotterdam). HEL (52°23'12.43"N, 6°27'15.25"E) is a RB site in the east of NL surrounded by rural areas. It is located around 150 km from SCH.

https://doi.org/10.5194/acp-2019-493
Preprint. Discussion started: 18 June 2019
© Author(s) 2019. CC BY 4.0 License.

Atmospheric Chemistry and Physics Discussions

Measurements of $PM_{2.5}$ chemically speciated data were available at the two sites during the period September 2007 – August 2008. A total of 479 samples were used in Mooibroek et al. (2011) for PMF analysis using data from 5 sites. 87 and 82 samples were collected at UB and RB, respectively. Table S3 reports the mean concentrations of $PM_{2.5}$ chemical species at these two sites.

- *Germany (DE)*

The PM chemically speciated data and the PMF source apportionments used here were published by van Pinxteren et al. (2016). Data from four stations (Leipzig-Mitte (LMI; TS), Leipzig Eisenbahnstrasse (EIB; TS), Leipzig TROPOS (TRO; UB), and Melpitz (MEL; RB) were collected during summer 2013 and winters 2013/14 and 2014/15. A total of 172 samples were used in the PMF model by van Pinxteren et al. (2016). In order to apply the PMF+Lenschow's approach, we excluded the TS (Leipzig-Eisenbahnstrasse) located in a residential area, approx. 2 km east of LMI. Below, a brief description of the three measuring sites used in this work, namely: the TS site in Leipzig (LMI; 51°20'39.0"N, 12°22'37.7"E), the UB site in Leipzig (TRO; 51°21'09.0"N, 12°26'05.0"E) and the RB station of Melpitz (MEL; 51°31'31.7"N, 12°55'40.6"E). LMI is an official monitoring site in the air quality network of the Saxon State Office for Environment, Agriculture, and Geology (LfULG). It is located next to a major crossroad in the center of Leipzig with a traffic intensity of approx. 40,000–50,000 vehicles per day. TRO is located at the TROPOS Institute on a science campus in an urban background area of Leipzig with a distance of 150 m to the next larger road. MEL is the RB TROPOS research site approximately 50 km north-east of Leipzig.

- *France (FR)*

Two sites were used: a UB site in *Lens* (LEN; 50°26'13"N, 2°49'37"E, 47 m a.s.l.) and the RB station of *Revin* (REV; 49°54'28.008"N, 4°37'48"E, 395 m a.s.l.). The distance between Lens and Revin is around 140 km. *LEN* (UB) site: The city of Lens (35,000 inhabitants) is actually part of a larger conurbation of more than 500,000 inhabitants and is surrounded by other large populated areas in northern FR (conurbation of Lille: 35 km northeast of Lens; Bethune: 27 km northwest of Lens, and Valenciennes: 58 km east of Lens). Since the sampling site is located relatively far away from major roads (approximately 1 km) and stationary emission sources, it is expected to be influenced by many anthropogenic activities (Waked et al., 2014). REV RB site is located in northeastern FR, close to the Belgian border. The air masses are mainly coming from the South-West but the site also experiences highly polluted air masses are advected

https://doi.org/10.5194/acp-2019-493
Preprint. Discussion started: 18 June 2019
© Author(s) 2019. CC BY 4.0 License.

Atmospheric Chemistry and Physics Discussions

from northern Europe. The site is classified as a background station and it is also considered as a remote site according to EMEP guidelines.

Measurements of PM_{10} chemically speciated data were available at the two sites during the period January 2013 – May 2014. A total of 335 samples (167 from LEN, and 168 from REV) were analyzed with PMF. The number of 24h samples simultaneously collected at the two sites and used for Lenschow's approach was 104. Table S4 reports the statistics of the chemical species measured at the French paired sites.

3. Results

This section is organized as follows: Section 3.1 presents the PMF sources calculated for each group of paired sites. Some of these sources were common for all the sites included in this work, whereas other sources were obtained only for a subset of paired sites. The chemical profiles of the sources calculated for ES, CH and FR are reported in Supporting Material (Figures S1, S2, and S3, respectively). The source chemical profiles for NL and DE can be found in Mooibroek et al. (2011) and van Pinxteren et al. (2016), respectively. In Section 3.2, we present a sensitivity study that aimed at demonstrating the feasibility of the multi-site PMF analyses. In Section 3.3, we present the PMF source contributions, and in Section 3.4, we present and discuss the results of the Lenschow approach applied to PM concentrations and PMF source contributions.

3.1 PMF sources

Sources identified at all paired sites

- *Secondary inorganic aerosol* (SIA) is the main component of fine particulate matter and has significant impacts on air quality, human health, and climate change (i.e. EEA, 2018; IPCC, 2013). This source was traced mostly by inorganic species: ammonium (NH_4^+), sulfate (SO_4^{2-}) and nitrate (NO_3^-). At all sites included here, with the exception of DE, we were able to separate the contribution of SIA between *sulfate-rich aerosols* (or secondary sulfate, SSA) and *nitrate-rich aerosols* (or secondary nitrates, NSA) which contributions peak in summer and winter, respectively. In DE, these two sources were not separated and the SIA source was obtained from PMF (van Pinxteren et al., 2016). The origin of SSA is the atmospheric oxidation of SO_2, mostly from combustion of sulfur-containing fuels. At all sites the SSA source profile (and consequently the SIA source profile in DE) showed relatively high contents of organic carbon (OC), which was attributed to the condensation of semi-volatile compounds on

https://doi.org/10.5194/acp-2019-493
Preprint. Discussion started: 18 June 2019
© Author(s) 2019. CC BY 4.0 License.

the high specific surface area of ammonium sulfate (Amato et al., 2009). Moreover, secondary OC is expected to be in receptor modelling studies largely associated with SSA because of the importance of photochemistry on the formation of both secondary types of aerosol particles, and consequently causing similar temporal variation of these constituents of atmospheric PM (Kim et al., 2003). SSA has its highest concentrations in the summer. NSA consists mainly of the secondary aerosol components NO_3^- and NH_4^+ and is thought to be mostly the semi-volatile ammonium nitrate. The origin of NO_3^- is the oxidation of NO_x emitted by combustion processes, mainly traffic, power generation, industry and domestic sector. The chemical profiles of this source were also enriched in OC. NSA has its highest concentrations in winter with generally low concentrations in summer because of the low summer thermal stability of ammonium nitrate (i.e. Stelson and Seinfeld, 1967).

- The *Mineral* source (MM) source was traced by typical crustal elements such as Al, Ca, Fe, and Mg. The MM source accounts for a large mass fraction of crustal trace elements such as Ti, Rb, Sr, Y, La, Ce and Nd. This factor also included a variable fraction of OC, an indication of mixing of inorganic and organic matter during aging or by entrainment of soils including their associated organic matter (Kuhn, 2007). At the German sites, this source (named *Urban dust* in van Pinxteren et al. (2016)) consisted of NO_3^- and WSOC (water soluble organic carbon) with high mass contributions of Ca and Fe indicating a mixture of mineral dust with urban pollution. A MM factor (enriched in Si, Al, Ti, Ca and Fe) was also detected by Mooibroek et al. (2011) in $PM_{2.5}$ at the Dutch sites.
- The *Primary road traffic* (RT) source was traced mainly by EC and OC and was associated with a range of metals such as Fe, Cu, Ba, Mo and Sb. This source included both exhaust and non-exhaust primary traffic emissions. The presence of trace metals in the chemical profiles indicated emissions from brakes and tires abrasion (i.e. Amato et al., 2009). Only for DE was possible to separate the contributions from exhaust and non-exhaust traffic emissions (van Pinxteren et al., 2016) whereas in the other cases, the two sources were jointly apportioned. In van Pinxteren et al. (2016), the vehicle exhaust emissions were identified by high mass contributions of WISC (water insoluble carbon; sum of EC and WISC), as well as contributions of hopanes with increasing species contributions toward either lower chain length (<C25) n-alkanes (for ultrafine particles) or larger (≥C25) chain length n-alkanes with a predominance of even C compounds (coarse particles). The contributions from exhaust and non-exhaust traffic sources in DE were summed to obtain the RT source contribution.

https://doi.org/10.5194/acp-2019-493
Preprint. Discussion started: 18 June 2019
© Author(s) 2019. CC BY 4.0 License.

Atmospheric Chemistry and Physics Discussions

462 - The *Sea salt* (SS) source was detected at all paired sites included in this
463 analysis. This source was traced mostly by Na^+ and Cl^- with contributions from SO_4^{2-}
464 and NO_3^- suggesting some aging of the marine aerosol. In CH, this source contributed
465 to high fractions of Na^+ and Mg^{2+} and did not show a clear annual cycle with elevated
466 values during winter, thus suggesting a low contribution from the de-icing road salt. In
467 Gianini et al. (2012), this source was named *Na-Mg-rich* factor and it was related to the
468 transport of sea spray aerosol particles in Zurich (Gianini et al., 2012). In DE, the
469 calculated SS factor consisted mainly of NO_3^- and Na^+ with no mass contribution of Cl^-,
470 indicating efficient Cl^- depletion by exchange with NO_3^-during transport over the
471 continent. In FR, two SS sources were calculated: a fresh SS source (traced by Na^+
472 and Cl^-), and an aged SS source with lack of Cl^- and presence of Na^+ and NO_3^-.
473
474 ***Sources identified only at a subset of paired sites***
475 - The *biomass burning* (BB) source was resolved for three paired sites (in FR,
476 DE, and CH). This source was mostly traced by K^+ and levoglucosan together with EC
477 and OC.
478 - The *residual oil combustion* source (V-Ni) was detected at two paired sites (in
479 ES and NL). This source contained significant fractions of the measured V and Ni
480 concentrations together with EC, OC and SO_4^{2-} that are the tracers for residual oil
481 combustion. Typical oil combustion sources are ocean shipping, municipal district
482 heating power plants, and industrial power plants using residual oil.
483 - The *primary industrial* (IND) source also detected only in ES and NL. In ES, it
484 was identified primarily by the high Pb and Zn concentrations along with As and Mn
485 representing emissions mostly from metallurgical operations (e.g. Amato et al., 2009).
486 In NL, different trace metals appeared indicating a mixture of many different sources,
487 including waste incineration, (coal) combustion, metallic industrial activities, and
488 fertilizer production. Mooibroek et al. (2011) summarized the profile as industrial
489 activities and incineration.
490
491 ***Sources identified at only one set of paired sites***

492 - Two sources were detected only in FR, namely: a m*arine biogen*ic (MB) source
493 identified by methane sulfonic acid, a product of DMS oxidation, and a *Land* (or
494 *primary*) *biogenic* source (LB), traced by alcohols (arabitol and mannitol).
495 - Six additional sources were detected only in DE: *sea salt/road salt* (SSRS)
496 factor with high mass contributions of Na^+ and Cl^- and higher values at the traffic site
497 indicating an influence of road salt for de-icing; *Coal combustion (CC)*, showing high

https://doi.org/10.5194/acp-2019-493
Preprint. Discussion started: 18 June 2019
© Author(s) 2019. CC BY 4.0 License.

Atmospheric Chemistry and Physics Discussions

mass contributions of WISC, NH_4^+, SO_4^{2-}, and WSOC and high species contributions of PAHs and As; *Local coal combustion*, (contributing mostly at EIB site, which was removed from this analysis) although the identification of this factor is tentative since its mass was mainly composed of nitrate instead of WISC. Species contributions of hopanes were very high with homohopane indices of 0.02 for ultrafine and ca. 0.25 for fine particles (i.e. closer to coal combustion than diesel values); *Photochemistry* (PHO), showed high mass contributions of $NH_4^+$and SO_4^{2-} and WSOC as well as high species contributions of oxalate. Other sources were; *Cooking*, with dominant mass contributions of WISC and WSOC; *Fungal spores*, with high mass contributions of carbonaceous material, also somewhat of NO_3^- and/or SO_4^{2-}. Arabitol is a unique tracer for fungal spores and showed very high species contributions. The carbon preference indexes of the n-alkanes were about 12 and thus clearly in the biogenic range (van Pinxteren et al., 2016). A detailed description of the additional sources obtained in DE can be found in van Pinxteren et al. (2016).

3.2 Feasibility of the multi-site PMF

Table 1 shows the main features of the sources from both the single-site PMF and the multi-site PMF for ES, CH, and FR. Table 1 reports for each source and country: the explained variation (EV) of the main markers of the source for each PMF run (i.e. how much each source explains in % the concentration of a given tracer); the ratio values (K) between specific tracers in each source for each PMF run; and the coefficient of variation (CV) of the ratios for each source (calculated as the ratio between the standard deviation and the mean of the K values obtained from the single-site PMF). This sensitivity test was not performed for NL and DE because the multi-site PMF was not applied here but directly taken from Mooibroek et al. (2011) and van Pinxteren et al. (2016), respectively. Given the encouraging results shown below for ES, CH, and FR, it seems valid to assume that the multi-site PMF results for DE and NL can be used, even without the single-site validation. As reported in Table 1, the calculated CVs are below 20-25% for the majority of the sources.

The exceptions were *IND* in ES (CV=48.8%), *SS* in ES (CV=35.9), *MB* in FR (CV=31.9%) and *RT* in CH (CV=31.1%). As shown below, the contribution of the *IND* source to the measured PM_{10} in BCN was very low and consequently the uncertainty associated to the high CV for this source was minimal. The high CV for the SS source in ES is due to the progressive depletion of Cl^- when moving from UB to RB and to CB. In fact, as reported in Table 1, the $[Na^+]/[Cl^-]$ ratio correspondingly increased when moving from the UB site to the CB site. However, the SS source, and the MB source,

https://doi.org/10.5194/acp-2019-493
Preprint. Discussion started: 18 June 2019
© Author(s) 2019. CC BY 4.0 License.

Atmospheric Chemistry and Physics Discussions

were considered as a natural sources without separating the urban and regional increments. Thus, the contribution from these two sources can be totally attributed to regional natural sources. On the other side, the RT source in CH was, as shown below, mostly local. For all other sources, the CVs are quite low indicating the similarity in the chemical profiles at the three sites, thereby allowing the application of the multi-site PMF.

Table 1: Main features of the sources from both the single-site PMF and the multi-site PMF (shaded background) for each country. EV: explained variation of the main markers of the sources for each PMF run; K: ratios between specific tracers in each source profile; CV: coefficient of variation of the ratios for each source. Ratio: ratios used to calculate K. CV values above 25% are highlighted in bold.

Source	Country	Paired sites	base run EV	K	CV [%] (a)	Ratio
SSA	Spain	BCN	SO_4^{2-} (48%), NH_4^+(41%)	0.233	13.7	$[NH_4^+]/[SO_4^{2-}]$
		MSY	SO_4^{2-} (35%), NH_4^+ (66%)	0.307		
		MSA	SO_4^{2-} (57%), NH_4^+ (51%)	0.280		
		BCN+MSY+MSA	SO_4^{2-} (49%), NH_4^+ (53%)	0.279		
	Switzerland	ZUE	SO_4^- (47%), NH_4^+ (27%)	0.389	9.3	
		PAY	SO_4^- (49%), NH_4^+ (26%)	0.444		
		ZUE+PAY	SO4- (56%), NH4+ (29%)	0.393		
	France	LEN	SO_4^{2-} (64%), NH_4^+ (28%)	0.348	0.2	
		REV	SO_4^{2-} (59%), NH_4^+ (33%)	0.347		
		LEN+REV	SO42- (74%), NH4+ (35%)	0.331		
NSA	Spain	BCN	NO_3^- (75%), NH_4^+ (59%)	0.207	13.0	$[NH_4^+]/[NO_3^-]$
		MSY	NO_3^- (73%), NH_4^+ (34%)	0.256		
		MSA	NO_3^- (75%), NH_4^+ (35%)	0.266		
		BCN+MSY+MSA	NO3- (82%), NH4+ (47%)	0.177		
	Switzerland	ZUE	NO_3^- (50%), NH_4^+ (52%)	0.400	20.4	
		PAY	NO_3^- (76%), NH_4^+ (55%)	0.299		
		ZUE+PAY	NO3- (65%), NH4+ (58%)	0.373		
	France	LEN	NO_3^- (66%), NH_4^+ (50%)	0.286	5.1	
		REV	NO_3^- (80%), NH_4^+ (54%)	0.266		
		LEN+REV	NO3- (78%), NH4+ (58%)	0.266		
Mineral	Spain	BCN	Al (85%), Ca (75%), Ti (71%), Rb (69%)	490	20.0	[Al+Ca]/[La+Rb]
		MSY	Al (87%), Ca (63%), Ti (84%), Rb (66%)	382		
		MSA	Al (89), Ca (51%), Ti (84%), Rb (68%)	333		
		BCN+MSY+MSA	Al (90%), Ca (59%), Ti	365		

https://doi.org/10.5194/acp-2019-493
Preprint. Discussion started: 18 June 2019
© Author(s) 2019. CC BY 4.0 License.

Atmospheric Chemistry and Physics Discussions

			(77%), Rb (70%)			
	Switzerland	ZUE	Al (71%), Ti (58%), Sr (75%)	28.5	15.9	[Al]/[Ti+Sr]
		PAY	Al (71%), Ti (61%), Sr (61%)	35.7		
		ZUE+PAY	Al (80%), Ti (65%), Sr (72%)	32.9		
	France	LEN	Al (84%), Ca (73%), La (49%), Rb (39%)	1590	2.4	[Al+Ca]/[La+Rb]
		REV	Al (80%), Ca (80%), La (42%), Rb (28%)	1644		
		LEN+REV	Al (81%), Ca (68%), La (46%), Rb (47%)	1484		
Primary Road Traffic	Spain	BCN	EC (73%), Cu (77%), Sb (79%)	9.35	18.7	[Cu]/[Sb]
		MSY	EC (58%), Cu (48%), Sb (46%)	13.51		
		MSA	EC (81%), Cu (40%), Sb (35%)	12.76		
		BCN+MSY+MSA	EC (75%), Cu (81%), Sb (80%)	9.31		
	Switzerland	ZUE	EC (46%), Cr (56%), Cu (47%), Sb(48%)	9.22	**31.1**	
		PAY	EC (36%), Cr (54%), Cu (38%), Sb(49%)	5.90		
		ZUE+PAY	EC (42%), Cr (60%), Cu (74%), Sb(69%)	9.39		
	France	LEN	EC (52%), Cu (51%), Sb (42%)	10.09	20.1	
		REV	EC (40%), Cu (53%), Sb (50%)	7.58		
		LEN+REV	EC (72%), Cu (60%), Sb (63%)	10.25		
Sea salt	Spain	BCN	Na^+ (80%), Mg_2^+ (41%), Cl^- (81%)	1.32	**35.9**	$[Na^+]/[Cl^-]$
		MSY	Na^+ (82%), Mg_2^+ (35%), Cl^- (61%)	2.19		
		MSA	Na^+ (72%), Mg_2^+ (25%), Cl^- (38%)	2.83		
		BCN+MSY+MSA	Na+ (83%), Mg2+ (38%), Cl- (83%)	1.34		
	Switzerland	ZUE	Na^+ (83%), Mg_2^+ (40%)	10.76	16.6	$[Na^+]/[Mg_2^+]$
		PAY	Na^+ (86%), Mg_2^+ (63%)	8.50		
		ZUE+PAY	Na+ (80%), Mg2+ (47%)	9.63		
Fresh sea salt	France	LEN	Cl^- (84%), Na^+ (55%), Mg_2^+ (49%)	0.547	2.5	$[Na^+]/[Cl^-]$
		REV	Cl^- (90%), Na^+ (44%), Mg_2^+ (40%)	0.567		
		LEN+REV	Cl- (87%), Na+ (42%), Mg2+ (36%)	0.508		
Aged sea salt	France	LEN	Na^+ (36%), Mg_2^+ (33%)	8.66	13.3	$[Na^+]/[Mg_2^+]$
		REV	Na^+ (45%), Mg_2^+ (38%)	10.46		

https://doi.org/10.5194/acp-2019-493
Preprint. Discussion started: 18 June 2019
© Author(s) 2019. CC BY 4.0 License.

Atmospheric Chemistry and Physics Discussions

		LEN+REV	Na+ (58%), Mg2+ (52%)	9.33		
Biomass burning	Switzerland	ZUE	EC (21%), K^+ (56%)	0.430	16.1	$[K^+]/[EC]$
		PAY	EC (29%), K^+ (41%)	0.342		
		ZUE+PAY	EC (32%), K+ (51%)	0.301		
	France	LEN	K^+(28), Levo. (82%), Polys. (85%)	7.15	23.5	[Levo.]/[Polys.]
		REV	K^+(33), Levo. (84%), Polys. (83%)	10.00		
		LEN+REV	K+(28), Levo. (89%), Polys. (85%)	8.58		
Residual Oil	Spain	BCN	V (69%), Ni (62%)	2.58	13.9	[V]/[Ni]
		MSY	V (61%), Ni (54%)	2.43		
		MSA (**)	V (42%), Ni (42%)	1.96		
		BCN+MSY+MSA	V (70%), Ni (62%)	2.57		
Primary industrial	Spain	BCN	Zn (75%), Pb (59%)	0.107	**48.8**	[Pb]/[Zn+As]
		MSY	Zn (75%), Pb (64%)	0.309		
		MSA	Zn (53%), Pb (52%)	0.205		
		BCN+MSY+MSA	Zn (75%), Pb (65%)	0.140		
Marine biogenic	France	LEN	Mg_2^+ (9%), MSA (74%)	0.114	**31.9**	$[Mg_2^+]/[MSA]$
		REV	Mg_2^+ (6%), MSA (81%)	0.072		
		LEN+REV	Mg2+ (3%), MSA (86%)	0.035		
Land biogenic		LEN	OC (10%), Alcohols (87%)	0.074	0.9	[Alcohol]/[OC]
		REV	OC (13%), Alcohols (82%)	0.075		
		LEN+REV	OC (9%), Alcohols (89%)	0.080		

(a) CV = (Standard Deviation / Mean) x 100

(**) Mixed with SSA in the single MSA PMF.

3.3 PMF source contributions and seasonal patterns

Figure 2 shows the mean annual PMF source contributions calculated for the considered paired sites. The mean winter (DJF) and summer (JJA) source contributions are presented in Figures S4 and S5, respectively, in the Supporting Material. Figure S6 in Supporting Material reports the same information as in Figure 2 but using box-and-whisker plots to show the data variability. Figures 3 and 4 show the annual cycle of the contributions to PM from the common sources and from those sources detected only at subsets of paired sites. The annual cycles of the sources obtained only in FR and DE are presented in Figure S7 in the Supporting Material.

At all stations, the secondary inorganic aerosol (SIA = SSA + NSA) was among the most abundant components of PM, especially for the Dutch stations where $PM_{2.5}$ was measured. At UB and RB stations in DE and FR (where the sampling periods were similar), the contribution to PM_{10} mass from SIA was comparable and around 5.7-5.8 $\mu g/m^3$ (29-35%) at UB sites and 3.3-4.4 $\mu g/m^3$ (24-37%) at RB sites.

https://doi.org/10.5194/acp-2019-493
Preprint. Discussion started: 18 June 2019
© Author(s) 2019. CC BY 4.0 License.

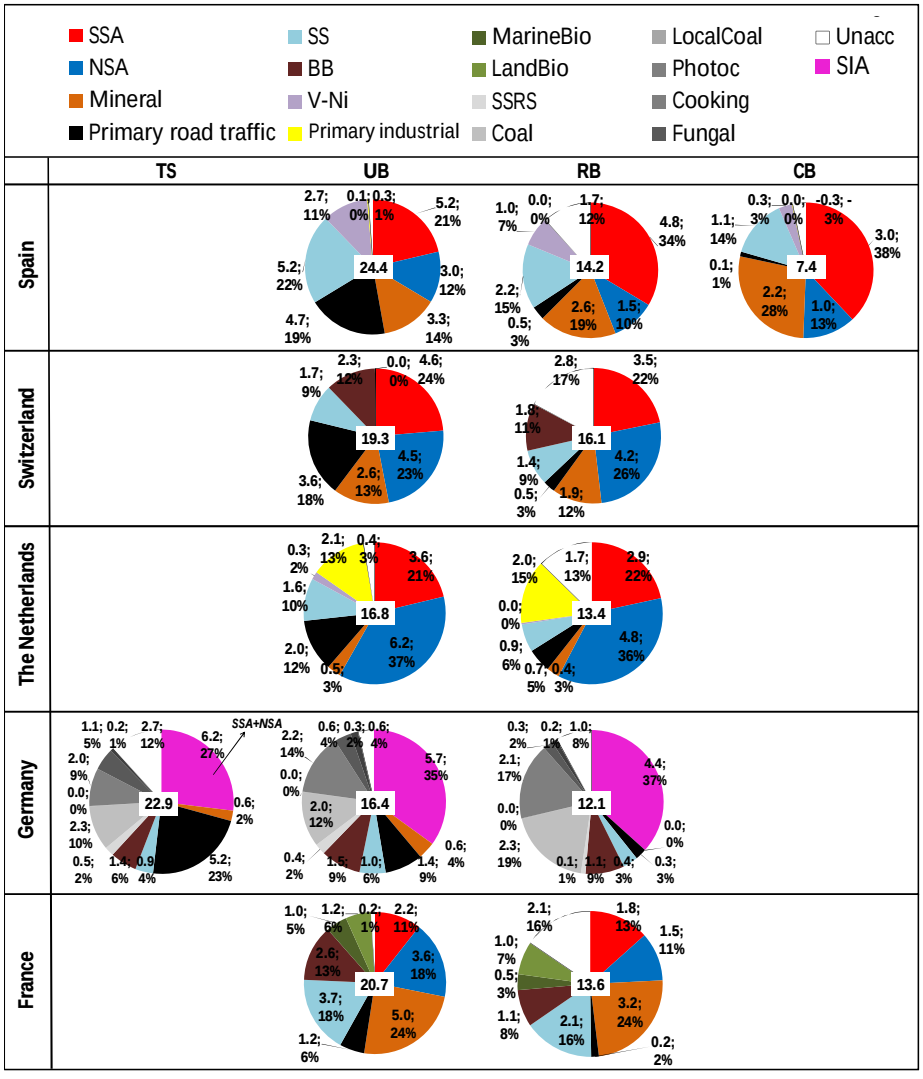

Figure 2: Mean annual source contributions to PM_{10} ($PM_{2.5}$ for NL) from the multi-site PMF for each country. The number in the white box at the center of the pie chart is the measured mass of PM (in $\mu g/m^3$). TS: traffic site; UB: urban background; RB: regional background; CB: continental background.

The SIA contribution reported here for LEN (UB, FR) was very similar to the value reported from Waked et al. (2014) at the same site over a different period. Higher values were obtained in ES, CH, and NL where the sampling periods were also similar. In these countries, the mean annual SIA contribution was around 8.2-9.8 $\mu g/m^3$ (33-58%) at UB stations and 6.3-7.7 $\mu g/m^3$ (48-58%) at RB stations.The absolute

https://doi.org/10.5194/acp-2019-493
Preprint. Discussion started: 18 June 2019
© Author(s) 2019. CC BY 4.0 License.

Atmospheric Chemistry and Physics Discussions

contribution from NSA source at UB stations was 4-5 times higher in winter compared to summer in all countries, except in CH were the winter NSA was 30 times higher compared to summer due to very low summer contributions from this source (cf. Figures S4 and S5).

The highest absolute NSA contribution to PM was observed in NL in both winter and summer. As reported in Mooibroek et al. (2011), the concentration of ammonia in the Dutch atmosphere is such that when sulfate is fully neutralized, a considerable amount is left to stabilize the ammonium nitrate even in summer.

On average, at both UB and RB stations the SSA contribution was higher in summer compared to winter by a factor of 1.6-1.9 in ES and CH and around 1.1-1.2 in FR whereas the summer/winter ratio was 0.6-0.7 in NL (cf. S4 and S5). As reported in Mooibroek et al. (2011), the almost flat seasonal pattern of SSA contribution at Dutch sites resembles the long-term average of sulfate. Moreover, as shown later, this may reflect a substantial impact of primary sulfate sources like ships in NL during the study period (2007-2008).

As presented in Figure 2, the contribution from SSA only slightly decreased when moving from TS/UB to RB/CB suggesting a regional character of this source. NSA contribution showed higher decreasing gradients compared to SSA indicating that both regional (i.e. agriculture) and local (i.e. road traffic) sources contributed to this factor. These spatial gradients will be discussed in more details in the next section.

The contribution from the MM source was rather high at the three Spanish sites (around 3.3 – 2.2 $\mu g/m^3$; 14 – 28% of PM_{10} mass). High contributions to PM_{10} were also observed in CH (2.6 – 1.9 $\mu g/m^3$; 13 – 12% of PM_{10} mass) and in FR (5.0 – 3.2 $\mu g/m^3$; 24% of PM_{10} mass). Lower absolute and relative MM contributions (0.5 – 0.4 $\mu g/m^3$; 3% of $PM_{2.5}$ mass) were calculated for NL, where $PM_{2.5}$ was sampled, and in DE (0.6 – 0.0 $\mu g/m^3$; 4-0% of PM_{10} mass). These regional differences could be also related to the intensity and regional impact of Saharan dust outbreaks which can be very different from one year to the other, thus also contributing to explain the observed regional variation of the MM source contributions (Alastuey et al., 2016). For the LEN UB site, Waked et al. (2014) reported lower contribution from the MM source (around 2.6 $\mu g/m^3$; 13% of PM_{10} mass) during the period 2011/2012. The higher MM source contribution reported here could be due to the different period used (2013/2014) and to the fact that during the winter season of 2011/2012, the cumulative precipitation in this French region was above the normal levels (Waked et al., 2014). Moreover, the high contribution from the MM source observed during March-April 2014 (cf. Figure 3), when the contribution reached daily means of more than 40 $\mu g/m^3$, could also explain the

https://doi.org/10.5194/acp-2019-493
Preprint. Discussion started: 18 June 2019
© Author(s) 2019. CC BY 4.0 License.

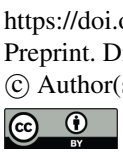

Atmospheric Chemistry and Physics Discussions

observed difference. Finally, van Pinxteren et al. (2016) reported that the contribution from the MM source at the German sites was much lower in winter compared to summer. For the German sites, we used data collected during one summer and two winters, thus also explaining the low annual average contribution from this source reported here. Low dust concentration in DE compared to other European countries was also reported by Alastuey et al. (2016).

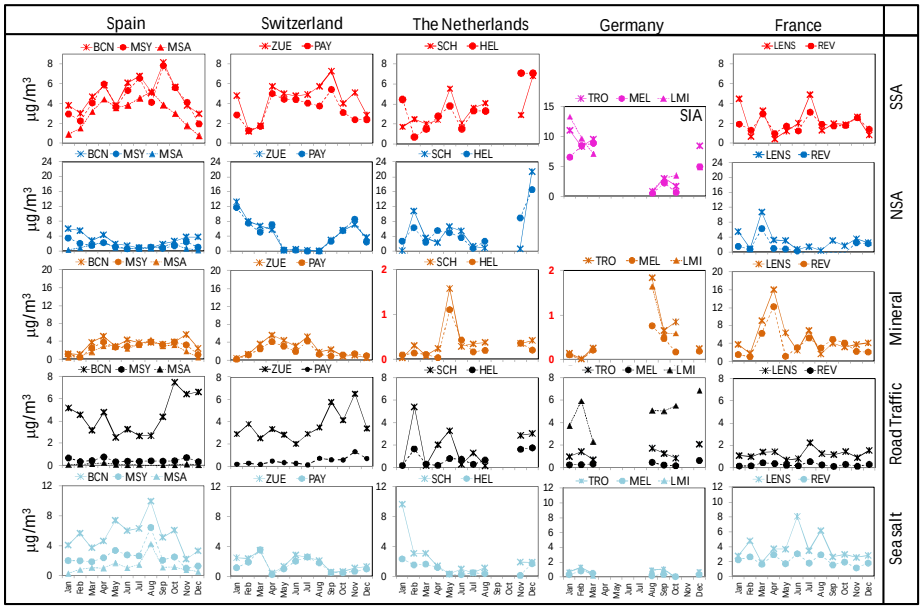

Figure 3: Annual cycles of the contributions from the common PM_{10} sources ($PM_{2.5}$ in NL) detected at all considered paired sites. Red color for the y-axis in the annual cycle plot of MM source contributions in NL and FR highlight different scales.

On average, higher contributions from the MM source were observed in summer compared to winter at all sites. The summer-to-winter ratio in ES and CH was similar and around 2.4-3.2 at UB stations and around 3.5 at RB level in both countries. This ratio was around 1-1.2 at UB stations in NL and FR and around 2-2.6 at RB stations. The highest summer-to-winter ratio for the MM source contribution was observed in DE where the ratio was around 11 and 8 at UB and RB, respectively. However, the contribution from this source was rather low in DE, thus increasing the uncertainty of the summer-to-winter ratio. As reported in Figure 2, a gradient was observed for the MM source contribution when moving from TS/UB to RB/CS. As for the NSA source,

https://doi.org/10.5194/acp-2019-493
Preprint. Discussion started: 18 June 2019
© Author(s) 2019. CC BY 4.0 License.

Atmospheric Chemistry and Physics Discussions

638 the observed spatial gradient for the MM source indicated both local and R+C
639 contributions to this source.
640 The mean annual contribution from the RT source was rather high at UB
641 stations in ES (4.7 μg/m^3; 19% of PM_{10} mass) and CH (3.6 μg/m^3; 18% of PM_{10} mass).
642 The contribution from this source was 2.0, 1.4, and 1.2 μg/m^3 at UB stations in NL, DE
643 and FR, respectively, corresponding to around 12%, 9%, and 6%, respectively, of PM
644 mass. The highest contribution from this source was observed at the TS in DE (5.2
645 μg/m^3; 23%) while the lowest value was observed at the CB site in ES (0.1 μg/m^3). The
646 absolute contributions at the RB sites were similar in all countries at around 0.2-0.7
647 μg/m^3 (2-5%). Thus, the RT source showed a clear gradient indicating that this source
648 was local at all TS/UB sites. In all UB sites, the RT source contribution was higher in
649 winter compared to summer, except at the UB sites in DE and FR were similar values
650 were obtained for both seasons. A similar result was reported by Waked et al. (2014)
651 for LEN (FR). The winter-to-summer ratio of the RT source contributions was around
652 0.9-1.1 in FR, DE, and CH whereas it was around 2 in ES increasing to 6 in NL,
653 suggesting different accumulation/dilution conditions in winter/summer in these two
654 latter countries.
655 The contributions from the SS source were highest at the paired sites close to
656 the sea such as in ES and FR were the mean annual contributions were around 5.2
657 μg/m^3 (22%) and 3.7 μg/m^3 (18%), respectively, at the UB stations. In both countries,
658 the mean annual contribution calculated at RB stations was lower compared to the
659 contribution at UB stations, because of the larger distance of RB stations to the sea
660 compared to the UB stations. In NL, SS contributed 1.6 μg/m^3 (10%) and 0.9 μg/m^3
661 (6%), at UB and RB stations, respectively. The lower SS contribution in NL compared
662 to ES and FR was due to the coarse mode prevalence of SS whereas $PM_{2.5}$ was
663 sampled in NL. In CH, the contributions from SS source were rather similar at UB and
664 RB stations and around 1.7 μg/m^3 (9%) and 1.4 (9%), respectively. The lowest
665 contributions from this source were observed at the German paired sites (0.4 – 1.0
666 μg/m^3). At all paired sites, with the exception of the Dutch paired sites, the SS source
667 contribution was higher in summer compared to winter. The summer-to-winter ratio
668 ranged from around 0.2 at UB and RB sites in NL to 1.8 in ES and FR. In the following,
669 we will not apply Lenschow's approach to the SS source contributions and we will
670 consider this source as totally natural and R+C in origin.
671 The contribution from the BB source was detected only in FR, DE, and CH.
672 Previous study in Barcelona using aerosol mass spectrometer data reported a small
673 BB contribution to OA and PM (around 11% and 4%, respectively) in winter in BCN

https://doi.org/10.5194/acp-2019-493
Preprint. Discussion started: 18 June 2019
© Author(s) 2019. CC BY 4.0 License.

Atmospheric Chemistry and Physics Discussions

(Mohr et al., 2012). Therefore, it was not possible to detect the BB source in BCN based on the PM_{10} chemical speciated data used here. BB contributions were similar in FR and CH and around 2.3-2.6 $\mu g/m^3$ (12-13%) and 1.1-1.8 $\mu g/m^3$ (8-11%) at UB and RB stations, respectively. The BB source contributions reported here for LEN site were very similar to the values reported by Waked et al. (2014) for LEN despite the differences in periods studied. In DE, the contributions were lower and ranged from 1.1 $\mu g/m^3$ (6%) to 1.4-1.5 $\mu g/m^3$ (6-9%) at RB and TS/UB sites, respectively. The contributions from this source were clearly higher in winter (cf. Figures S4 and S5). A slight gradient is observed moving from TS/UB to RB stations indicating the presence of both local and R+C increments for this source.

The V-Ni source contributions were higher in ES compared to NL at both UB and RB stations. This factor was not apportioned in the other countries. In FR because the measurements of V and Ni were not available; in DE only the measurements of Ni were available (whereas V, as important tracer of residual oil combustion was not available); in CH, despite the fact that the measurements of V were available, the V-Ni source was not detected likely because the distance of Swiss sites from important residual oil combustion sources. At the UB station in ES, the contribution from this source was around 2.7 $\mu g/m^3$ (11%) due to ship emissions from both the intense vessel traffic from the Mediterranean Sea and the port of Barcelona. At the Spanish RB and CB stations, the contributions from this source were reduced to around 1.0 $\mu g/m^3$ (7%) and 0.3 $\mu g/m^3$ (3%), respectively. The contributions were much lower at the UB station in NL (0.3 $\mu g/m^3$; 2%). In ES, this source contributed more in summer compared to winter with summer-to-winter ratio ranging from 3 at the UB site to 30 at the CT site likely due to the increase of cruise ships together with the intense sea breeze circulation in summer and the photochemistry, which enhances the SO_2 oxidation. Figure S8 shows the Concentration Weighted Trajectory (CWT) plots for the V-Ni source contributions in Barcelona (2010-2014) and Schiedam (2007-2008). The use of computed concentration fields to identify source areas of pollutants, referred as CWT, was first proposed by Siebert et al. (1994). Here, we used the CWT function available in the Openair package (Carslaw and Ropkins, 2012; Carslaw, 2012). In Figure S8, contributions higher than the 90^{th} percentile were used to look at the origin of high contributions from the V-Ni source. As shown in Figure S8, the V-Ni source in ES and NL was mostly linked to maritime shipping emissions.

Figure S9 in Supporting Material shows the scatter-space plots of the V-Ni and SSA source contributions for BCN (PM_{10}; 2007-2008 and 2010-2014) (Figure S9 c and d, respectively) and SCH ($PM_{2.5}$; 2007-2008; Figure S9 a). Data from Rotterdam ($PM_{2.5}$;

https://doi.org/10.5194/acp-2019-493
Preprint. Discussion started: 18 June 2019
© Author(s) 2019. CC BY 4.0 License.

Atmospheric Chemistry and Physics Discussions

2007-2008; Figure S9 b) were also used for the V-Ni vs. SSA comparison. Figure S9 also shows the analogous plots for 4 additional sites in NL, Belgium, and FR for a more recent period (2013-2014), namely: Wijk aan zee and Amsterdam in NL (Figure S9 e,f), Antwerp (Belgium, Figure S9 g) and Lille (FR, Figure S9 h). Details on the measurements performed at these 4 additional sites, the PM_{10} chemically speciated data, and PMF analyses can be found in Mooibroek et al. (2016). In all of the g-space plots in Figure S9, an edge was observed (highlighted with red color) that can be used to estimate the amount of SSA produced for every 1 $\mu g/m^3$ of residual oil burned by ships (e.g. Kim and Hopke, 2008; Pandolfi et al., 2011a). This sulfate represents direct SO_3 emissions from the ship that appear as particulate sulfate at the sampling sites. Ship diesels typically burn high sulfur content residual oil (Bunker-C), and thus primary sulfate emissions can be anticipated (Kim and Hopke, 2008). In BCN we found that around 0.4 $\mu g/m^3$ of SSA were produced for every 1 $\mu g/m^3$ of V-Ni PM_{10} contribution (during both 2007-2008 and 2010-2014), whereas in SCH and Rotterdam the amount of SSA was much higher, around 5.6-6.0 $\mu g/m^3$, suggesting the use of a residual oil with high sulfur content during 2007-2008. Kim and Hopke (2008) and Pandolfi et al. (2011a) reported that around 0.8 $\mu g/m^3$ of SSA were produced for every 1 $\mu g/m^3$ of V-Ni $PM_{2.5}$ in Seattle (US) and of V-Ni PM_{10} in the Bay of Gibraltar (ES), respectively. The difference between BCN and SCH and Rotterdam was high during the same period (2007-2008). However, recent data (2013-2014) from the four additional sites slowed lower primary SSA produced (around 0.8 – 1.5 $\mu g/m^3$) for every 1 $\mu g/m^3$ of residual oil, indicating a reduction of sulfur content in fuels (cf. Figure S9). Indeed, Figure S10 shows the strong reduction of SO_2 emitted from maritime shipping in Rotterdam from 2007 to 2014 despite the rather constant number of ships registered in port (Environmental Data Compendium, Government of the Netherlands, https://www.clo.nl/en). Moreover, a report of the Netherlands Research Program on Particulate Matter (Denier van der Gon and Hulskotte, 2010) reported that in the port of Rotterdam in 2003 the dominant energy source for ships in berth was high-sulfur content heavy fuel oil (HFO). The use of HFO in berth was a surprising result, as it is often thought that ships use distilled fuels while in berth (Denier van der Gon and Hulskotte, 2010). The observed reduction in primary SSA from ships in NL from 2007-2008 to 2013-2014 could be also due to the change of fuel used by ships in berth, from HFO to low-sulfur content marine diesel oil. The type of fuel used by ships while in berth could also explain the difference observed between BCN and SCH during 2007-2008.

https://doi.org/10.5194/acp-2019-493
Preprint. Discussion started: 18 June 2019
© Author(s) 2019. CC BY 4.0 License.

Atmospheric Chemistry and Physics Discussions

745 The contribution from the IND source was relatively higher in NL at around 2
746 μg/m^3 at UB and RB stations corresponding to 13% and 15% of the $PM_{2.5}$ mass. In ES,
747 the contribution from this source was very low (around 0.1 μg/m^3 at the UB station).
748 The implementation of the IPPC Directive (Integrated Pollution Prevention and Control)
749 in 2008 in ES is the most probable cause for the low contribution from the IND source
750 (Querol et al., 2007). As reported in Figure 2, a very small gradient was observed when
751 moving from UB to RB station suggesting a regional character for this source. In NL the
752 contribution from this source was higher in summer with a summer-to-winter ratio of
753 around 1.3-1.4 at both stations.
754
755

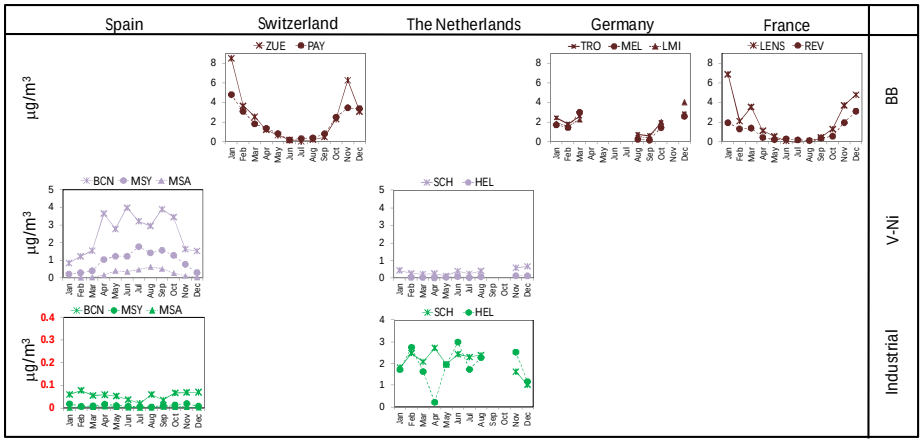

756
757 **Figure 4**: Annual cycles of the contributions to PM_{10} ($PM_{2.5}$ in NL) from BB, V-Ni and Industrial
758 sources.
759
760

761 Finally, the MB and LB sources, assessed only in FR, contributed around 1.0 μg/m^3
762 and 1.2 μg/m^3, respectively, at the UB station and 0.5 μg/m^3 and 1.0 μg/m^3,
763 respectively, at the RB station. These two sources were not detected in the other
764 countries mostly because the measurements of methane sulfonic acid and traced
765 alcohols (arabitol and mannitol) were not available.

766 These two sources combined explained around 7% and 10% of PM_{10} mass at
767 the UB and RB stations, respectively. The contributions from these two sources were
768 much higher in summer especially for the MB source when marine primary productivity
769 is maximum. Analogously to the SS source, Lenschow's approach was not applied to
770 the contributions from these two sources that were considered as totally R+C and
771 natural.

https://doi.org/10.5194/acp-2019-493
Preprint. Discussion started: 18 June 2019
© Author(s) 2019. CC BY 4.0 License.

Atmospheric Chemistry and Physics Discussions

In DE, the contributions from the six sources assessed only in this country summed to mean values of 6.1 μg/m^3 (26%), 5.6 μg/m^3 (34%), and 4.9 μg/m^3 (41%) at TS, UB and RB, respectively. Among these six sources, the contribution from CC was the highest in winter (suggesting the influence of buildings heating), explaining around 60-70% of the total contributions from these six sources. In summer, PHO was the source contributing mostly to the total from the six sources (50-80%). Among these six sources, only the contribution from the *fungal spores* source was considered as totally R+C and natural.

3.4 Spatial increments: Lenschow`s approach results

The results of Lenschow's approach applied to the PM mass concentrations and to the PMF source contributions for each country are presented in Figure 5 and Table S5 and Figure 6 and Table S6, respectively. Figures 5 and 6 show the annual average values. Allocation of PM concentrations and source contributions for winter (DJF) and summer (JJA) are presented in Figures S11 and S12 and Table S5, for PM concentrations, and in Figures S13 and S14 and Table S7 and Table S8, for the PMF source contributions.

An attempt was made to separate the natural and anthropogenic R+C increments whereas the urban increment was considered to be totally anthropogenic. We considered some sources such as *sea salt*, *aged sea salt*, *marine biogenic*, *land biogenic* as totally natural without allocating their contributions to the different spatial levels. Thus, for example, we assumed that there were no local (traffic/urban) sources of *sea salt*. For the *aged sea salt* source the presence of SIA in the chemical profile suggests that this source was not entirely natural. However, we cannot estimate the relative natural and anthropogenic contributions to this source using data available here. The urban MM increment was associated with resuspended dust from passing vehicles and local demolition/construction activities. Consequently, it was considered anthropogenic in origin. Conversely, the R+C MM increment was considered to be as of natural origin from both wind-blown dust and Saharan dust episodes, the latter being most important in the Mediterranean region and especially in summer compared to other European countries (Pey et al., 2013; Alastuey et al., 2016). Nevertheless, regional suspended soil could be the result of anthropogenic activities such as farming. However, it is impossible based on the available information to estimate the relative contributions of natural and anthropogenic sources to the R+C MM increments. Other sources such as SSA and NSA, RT, IND, V-Ni, and BB, were considered

https://doi.org/10.5194/acp-2019-493
Preprint. Discussion started: 18 June 2019
© Author(s) 2019. CC BY 4.0 License.

anthropogenic in origin. Finally, the gradients of PM concentrations reported in Figure 5 and Table S5 were calculated by summing the increments calculated from the different source contributions, and not as the difference between the gravimetric measurements performed at the paired sites.

3.4.1 Urban and regional-continental PM allocation

As reported in Figure 5, the sum of the annual natural and anthropogenic R+C PM increments in all countries were higher compared to the urban increments, therefore confirming the statement of the 2016 LRTAP Assessment Report about the importance of long range air pollution, even in urban areas. On annual basis, the relative R+C PM_{10} increments were similar in all countries and ranged between around 64% in ES to 74% in DE (cf. Table S5), For this comparison, the R+C PM increment in ES was calculated as the sum of regional and continental increments and in DE it was calculated as relative to the PM_{10} concentration measured at the UB site (not at the LMI traffic site). If the relative R+C PM_{10} increment in DE is calculated with respect to the PM_{10} mass measured at LMI traffic site, then the R+C increment can be estimated to be around 55% in close agreement with the R+C PM_{10} increment reported by van Pinxteren et al. (2016). For NL, the relative R+C $PM_{2.5}$ increment was around 74%, whereas in CH and FR, the relative R+C PM_{10} increments were around 67-69%.

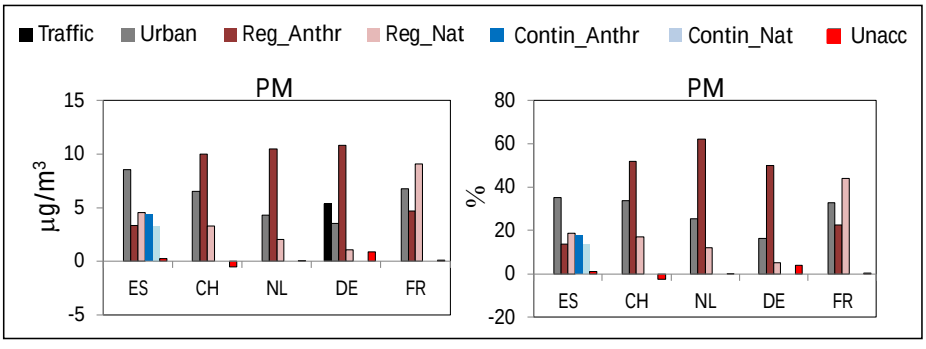

Figure 5: Lenschow's approach applied to the concentrations of PM_{10} in the different countries ($PM_{2.5}$ in the Netherlands). Annual means are reported. ES: Spain; CH: Switzerland; NL: The Netherlands; DE: Germany; FR: France. In all countries with the exception of Spain, Reg_Anthr and Reg_Nat are the sum of regional+continental.

https://doi.org/10.5194/acp-2019-493
Preprint. Discussion started: 18 June 2019
© Author(s) 2019. CC BY 4.0 License.

Atmospheric Chemistry and Physics Discussions

In terms of absolute values, the lowest PM urban and R+C (anthropogenic and natural) increments were observed in DE (3.5 μg/m^3 and 11.9 μg/m^3 of PM_{10} mass measured at the UB TRO site) where the PM_{10} concentrations were also lower compared to the other cities included in this work. The highest urban and R+C PM increments were instead observed in ES (8.5 μg/m^3 and 15.6 μg/m^3 of PM_{10} mass measured in BCN) where the PM_{10} concentrations were higher. For DE, the local PM increment measured at the traffic site (LMI) was 5.4 μg/m^3 (cf. Table S5) and contributed around 25% to the PM mass measured at LMI.

Overall (annual means; cf. Table S5 and Figures 5, S11, and S12), the R+C PM increments due to anthropogenic activities in CH, NL, and DE were higher compared to the R+C PM increment due to natural sources. In these countries, the R+C anthropogenic PM increments were very similar (10-10.8 μg/m^3) and explained around 52%, 62%, and 66%, respectively, of the PM mass measured at the UB stations. Conversely, in these three countries, the R+C PM increments due to natural sources varied more (1.1-3.3 μg/m^3) and explained around 17%, 12% and 7%, respectively, of the UB PM mass. In ES, the anthropogenic and natural R+C PM increments were similar (around 8 μg/m^3) and both explained around 32-33% of the PM mass measured at BCN. Conversely, in FR, the R+C natural PM increment was the highest (around 9.1 μg/m^3) and explained around 44% of the PM mass measured in LEN, whereas the R+C anthropogenic PM increment was around 4.6 μg/m^3 (23%). As shown later, the high R+C natural PM increment observed in FR and ES was mostly related to regional emissions from SS and MM sources. Moreover, in FR, *marine biogenic* and *land biogenic* source emissions also contributed to the high R+C natural PM increment.

In all countries, with the exception of DE, the absolute and relative PM urban increments were higher in winter compared to summer (cf. Table S5). This result suggested that in winter, the typical atmospheric conditions in these countries of lower wind speeds and lower mixed layer heights favored the accumulation of locally emitted pollutants compared to summer. The winter-to-summer PM urban increment ratios ranged between 1.5 in CH up to 3.5 in FR. The lack of a clear seasonal profile for the PM urban increment at TRO (DE) could be due to the overall effect that the two main air mass inflows have on pollutant concentrations at the German sites during both seasons (van Pinxteren et al., 2016). As shown in van Pinxteren et al. (2016), the source contributions to PM at the German sites differed considerably depending on the sources, seasons, and air mass inflows.

The natural and anthropogenic R+C PM increments showed different seasonal patterns. Those due to natural sources were higher in summer at all sites with the

https://doi.org/10.5194/acp-2019-493
Preprint. Discussion started: 18 June 2019
© Author(s) 2019. CC BY 4.0 License.

exception of NL where the R+C natural PM increment was higher in winter. As shown later, the observed higher summer R+C PM natural increments were due to MM and SS source emissions that were higher on average during the warm season. Conversely, as also shown in Waked et al. (2014), the high R+C PM natural increment in NL in winter was due to SS emissions that were higher during the cold season (cf. Tables S7 and S8).

The R+C PM increments due to anthropogenic sources showed an opposite seasonal profile compared to the R+C natural PM increments. In fact, the anthropogenic R+C PM increments were lower in summer compared to winter in all countries, with the exception of ES where it was higher in summer compared to winter. As shown later, the higher anthropogenic R+C PM increment in summer in ES was mostly driven by high contributions from regional SSA sources, mostly related to ship emissions at the Spanish sites, and the peculiar meteorological patterns in the Western Mediterranean inducing vertical recirculation of air masses (i.e. Millán et al., 1997). The relatively lower anthropogenic R+C PM increment observed in the other countries in summer compared to winter were mostly related to high winter contributions from NSA and BB regional sources.

3.4.2 Allocation of PMF source contribution

- Sources identified at all paired sites

SIA source (anthropogenic)

In all countries, the majority of SIA calculated from PMF was of R+C origin (Figure 6). On annual average, the lowest relative R+C SIA increment was around 57% in FR (where 43% of *SIA* was of local origin). In the other countries, the relative R+C SIA increment was similar and ranged between around 76% and 85% in ES and CH, respectively. In absolute values, the highest R+C SIA increment (around 7.7 $\mu g/m^3$; cf. Table S6) was observed in CH and NL, followed by ES (6.2 $\mu g/m^3$), DE (4.4 $\mu g/m^3$) and FR (3.3 $\mu g/m^3$). The relative R+C SIA increments were similar in winter and summer in all countries with the exception of ES where in summer the relative R+C SIA increment (around 88%; cf. Figure S14 and Table S8) was much higher compared to winter (51%; cf. Figure S13 and Table S7). In summer, the Western Mediterranean Basin is characterized by regional recirculation episodes driven by strong insolation and the orography of the area. These conditions in summer favor the formation of cells of meso-to-regional scales (i.e. Millan et al., 1997; 2000) and air mass recirculate over the region causing dispersion and aging of pollutants. Furthermore, the high summer insolation favors a faster oxidation of SO_2 and, accordingly, higher SO_4^{2-} concentrations

https://doi.org/10.5194/acp-2019-493
Preprint. Discussion started: 18 June 2019
© Author(s) 2019. CC BY 4.0 License.

Atmospheric Chemistry and Physics Discussions

(i.e. Querol et al., 1999). During these summer conditions, the SIA concentrations were similar at the three Spanish sites, thus leading to high relative R+C SIA contributions in summer compared to winter in ES (cf. Figures S4 and S5).

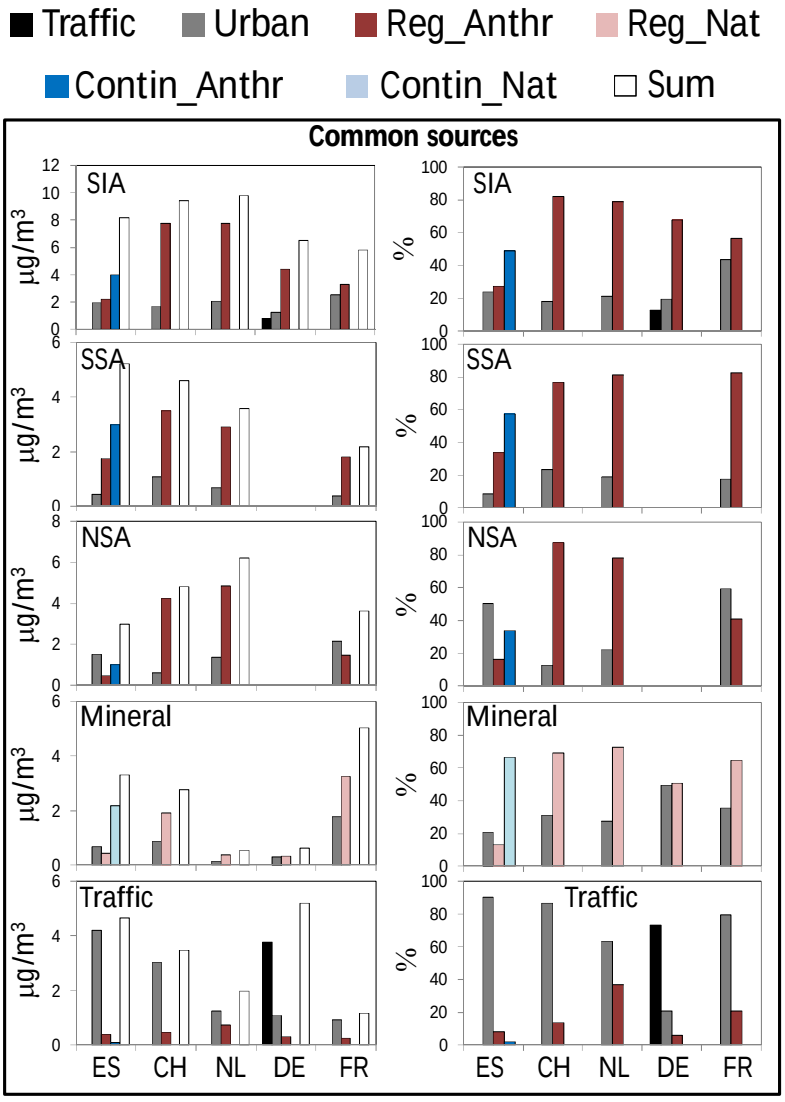

Figure 6: Lenschow's approach applied to the PM_{10} ($PM_{2.5}$ in the Netherlands) PMF source contributions. Annual means are reported. ES: Spain; CH: Switzerland; NL: The Netherlands; DE: Germany; FR: France. In all countries, with the exception of Spain, Reg_Anthr and Reg_Nat are the sum of regional+continental.

https://doi.org/10.5194/acp-2019-493
Preprint. Discussion started: 18 June 2019
© Author(s) 2019. CC BY 4.0 License.

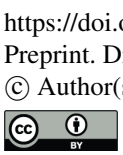

Atmospheric Chemistry and Physics Discussions

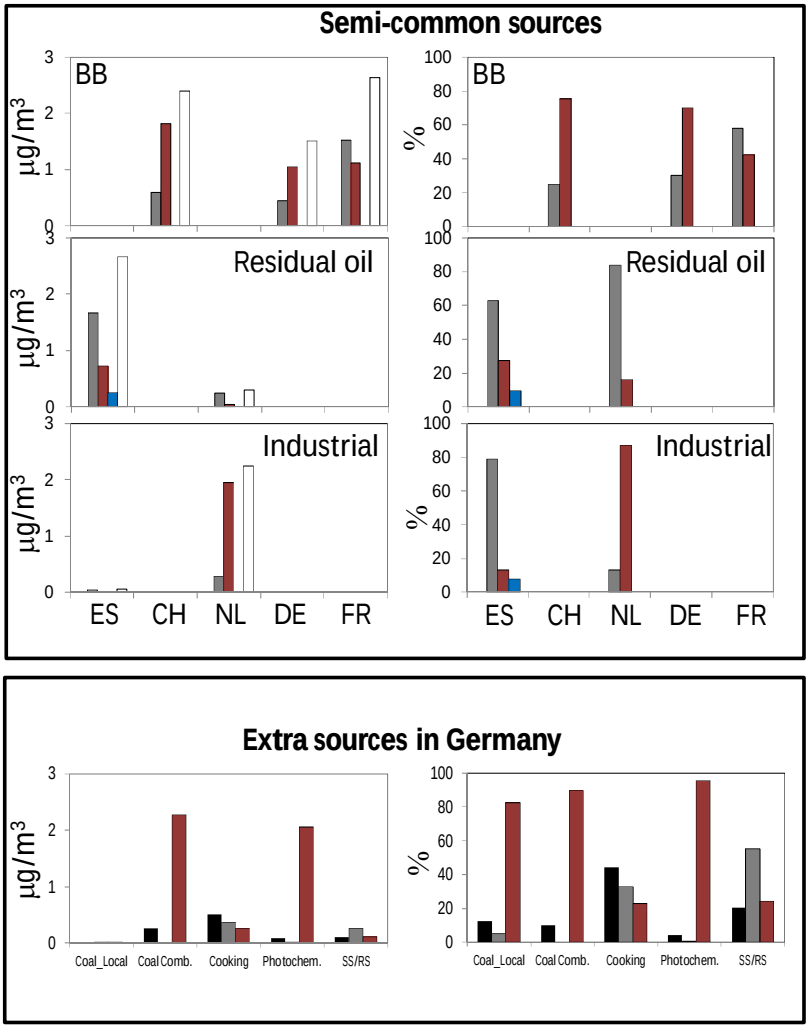

Figure 6 (continue): Lenschow's approach applied to the PM_{10} ($PM_{2.5}$ in the Netherlands) PMF source contributions. Annual means are reported. ES: Spain; CH: Switzerland; NL: The Netherlands; DE: Germany; FR: France. In all countries, with the exception of Spain, Reg_Anthr and Reg_Nat are the sum of regional+continental.

In absolute values, the R+C SIA increments were higher in winter compared to summer in all countries, with the exception of ES. The winter-to-summer R+C SIA increment ratios (using absolute values) ranged between 1.5 in FR to around 5 in DE. In ES it was 0.7. As shown later, the difference observed between ES and the other countries was due to the different effects that SSA and NSA have on the seasonal SIA profile. In ES, the higher relative and absolute R+C SIA increments in summer

https://doi.org/10.5194/acp-2019-493
Preprint. Discussion started: 18 June 2019
© Author(s) 2019. CC BY 4.0 License.

Atmospheric Chemistry and Physics Discussions

933 compared to winter were due to the increase of the R+C SSA increment during the
934 warm season. In the other European countries, the higher winter R+C SIA increment
935 compared to summer was due mostly to the strong increase of the NSA regional
936 increment during the cold season. The very high winter-to-summer R+C SIA increment
937 ratio observed in DE were likely related to the air mass transport at the German sites.
938 As reported by van Pinxteren et al. (2016), in DE during both summer and winter two
939 air mass origins prevail: western and eastern inflow. Particle mass concentrations in
940 Leipzig were typically higher during eastern than during western inflow and especially
941 during the winter period, thus explaining the high winter-to-summer ratio of the R+C
942 SIA increment in DE. This trend has been commonly observed in the area of Leipzig
943 and can be explained with a more continental character of eastern air masses (western
944 air masses typically spend considerable time above the Atlantic Ocean) and higher PM
945 pollution in Eastern European countries (e.g. Pokorná et al., 2013; 2015).
946
947 *SSA source (anthropogenic)*
948 As expected, the majority of SSA measured in the selected cities was of R+C
949 origin. On annual basis, the highest R+C SSA increment was observed in ES (4.8
950 μg/m^3, 91% of *SSA* source contribution in BCN). Thus, in BCN the local SSA increment
951 was low (0.5 μg/m^3; 9%). The high R+C SSA increment in ES was likely due to
952 shipping emissions in the Mediterranean Sea, whereas the very local SSA increment
953 could be linked to the emissions of primary sulfate from ships in the port of Barcelona
954 and the high concentrations of NH_3 measured in the city (Reche et al., 2012; Pandolfi
955 et al., 2012). Recently, Van Damme et al. (2018) identified Catalonia (NE Spain) as
956 one of the major hotspots in terms of NH_3 emissions. In all other countries, the annual
957 R+C SSA increment was lower and ranged between 3.5 μg/m^3 (77% of SSA source
958 contribution) in CH and 1.8 μg/m^3 (83%) in FR where the lowest absolute R+C SSA
959 increment was observed. The R+C SSA increment in NL, where the NH_3 emissions are
960 high (Van Damme et al., 2018), was estimated to be around 2.9 μg/m^3 (81% of SSA),
961 being the remaining SSA associated with primary emissions from ships. The relatively
962 high annual urban SSA increment observed at ZUE (CH; 1.1 μg/m^3; 24% of SSA
963 contribution in ZUE; cf. Figure 6 and Table S6) could be related to local road traffic and
964 wood combustion emissions which in addition contribute to NSA and SSA through
965 emissions of gaseous precursors of SIA (Gianini et al., 2012). In the other cities
966 included in this analysis, the local SSA increment ranged between 0.4 (LEN, FR) and
967 0.7 (SCH, NL) μg/m^3 (0-18%).

https://doi.org/10.5194/acp-2019-493
Preprint. Discussion started: 18 June 2019
© Author(s) 2019. CC BY 4.0 License.

Atmospheric Chemistry and Physics Discussions

In absolute values, the R+C SSA increment in summer was higher compared to winter in all countries with the exception of NL where a higher R+C SSA increment was observed in winter (4.0 $\mu g/m^3$) compared to summer (2.6 $\mu g/m^3$). Mooibroek et al. (2011) reported a flat seasonal pattern of the SSA source contributions in NL that resembled the long-term average of SO_4^{2-}. Moreover, the low SSA summer-to-winter ratio in the Netherland could be also associated with emissions of primary sulfate from ships, which, as shown before, was high in SCH during the period considered. In ES, the R+C SSA increment in summer (cf. Table S8) was related to long-range transport of SSA, which accumulated over the region due to the summer regional recirculation described above, and the photochemistry which enhances the SO_2 oxidation. .

Finally, in all countries the *SSA* absolute local increments did not show clear seasonal cycles likely resembling the effect of local sources on SSA.

NSA source (anthropogenic):

On annual average, high and similar R+C NSA increments were observed in CH (annual mean: 4.2 $\mu g/m^3$; 94% of NSA contribution in ZUE) and NL (4.8 $\mu g/m^3$; 78% of NSA contribution in SCH). Conversely, lower R+C NSA increments were observed in ES (1.5 $\mu g/m^3$; 50% of NSA contribution in BCN) and FR (1.5 $\mu g/m^3$; 41% of NSA contribution in LEN). In BCN (ES), the high local NSA increment (around 50% or 1.5 $\mu g/m^3$ of NSA source contribution in BCN) was explained by the NO_x emissions from traffic and the availability of NH_3 in the city of Barcelona (e.g. Reche at al., 2012; Pandolfi et al., 2012). High NO_x emissions originating from road traffic could also be responsible for the high local NSA increment in LEN (FR; 2.1 $\mu g/m^3$; 59% of NSA contribution to PM_{10} in LEN). Agricultural emissions of NH_3 and NO_x emissions from road and maritime traffic and industry were the likely cause of the high R+C NSA increment observed especially in NL and CH.

In all countries, as a consequence of the thermal instability of ammonium nitrate, both local and R+C NSA increments were higher in winter compared to summer (Figures S13 and S14 and Tables S7 and S8). In both winter and summer, the highest local and R+C NSA increments were observed in NL. In this country, the mean R+C NSA increments were 10 $\mu g/m^3$ and 2.5 $\mu g/m^3$ in winter and summer, respectively. The high summer R+C NSA increment in NL (much higher compared to the other countries where it was around of 0-0.8 $\mu g/m^3$) was due to the high concentration of NH_3 in the Dutch atmosphere and NO_x emissions. NH_3 concentration is such that when SSA is fully neutralized, a considerable amount is left to stabilize the ammonium nitrate also in summer (Mooibroek et al., 2011).

https://doi.org/10.5194/acp-2019-493
Preprint. Discussion started: 18 June 2019
© Author(s) 2019. CC BY 4.0 License.

Atmospheric Chemistry and Physics Discussions

Mineral (local anthropogenic; regional+continental natural):

On annual basis, the R+C MM increments were higher compared to the local increments at all sites with the exception of DE where the urban and R+C increments were similar. As reported in van Pinxteren et al. (2016), the MM factor identified in DE was characterized by high nitrate fraction and anthropogenic n-alkanes signature indicating a mixture of soil with urban pollution thus likely explaining the lower R+C increment compared to the other sites. Moreover, the seasonal and site dependencies of concentrations presented in van Pinxteren et al. (2016) suggested an urban background MM source without direct association to traffic. This could be the reason for the null traffic MM increment reported here for the German traffic site (Figure 6 and Table S6). The highest urban and R+C MM increments were observed in FR (1.8 $\mu g/m^3$ and 3.2 $\mu g/m^3$, respectively) followed by ES (0.7 $\mu g/m^3$ and 2.6 $\mu g/m^3$, respectively) and CH (0.9 $\mu g/m^3$ and 1.9 $\mu g/m^3$, respectively), whereas these values were much lower in NL (where $PM_{2.5}$ was sampled) and DE. For LEN (FR), Waked et al. (2014) showed a very similar trend for the MM factor and for primary traffic emissions in Lens, suggesting a major influence of road transport for particles resuspension. Alastuey et al. (2016) have shown that in the North of FR, the average mineral dust concentration and its relative contribution to PM_{10} was higher compared to DE and mostly in summer.

As shown in Figure 6, the majority of the R+C MM increments in ES were of continental origin (2.2 $\mu g/m^3$ continental and 0.4 $\mu g/m^3$ regional; cf. Table S6) and especially in summer (3.2 $\mu g/m^3$ continental and 0.1 $\mu g/m^3$ regional) whereas in winter the regional and continental contributions were lower and similar (0.4 $\mu g/m^3$ continental and 0.5 $\mu g/m^3$ regional). The seasonality of the MM increments observed in ES was also due to the long-range transport of mineral dust from the Saharan Desert during Saharan dust outbreaks (Querol et al., 2009; Pey et al., 2013). As shown in Alastuey et al. (2016), the contribution from desert dust to PM is expected to be higher in the Mediterranean region compared to Central/North of Europe. The higher R+C MM increments in summer compared to winter, observed also in the other countries, were linked to the enhanced regional resuspension of dust during the dry season together with Saharan dust outbreaks which are more sporadic in Central and North Europe (i.e. Gianini et al., 2102).

Road traffic (anthropogenic)

As expected, the majority of the RT source emissions were of local origin in all cities included in this analysis. The relative urban RT increments ranged between 62%

https://doi.org/10.5194/acp-2019-493
Preprint. Discussion started: 18 June 2019
© Author(s) 2019. CC BY 4.0 License.

Atmospheric Chemistry and Physics Discussions

in SCH (NL) to 90% in BCN. The relatively high R+C RT increment observed in NL (36% compared to 6-20% in the other countries) was in agreement with the value reported by Mooibroek et al. (2011). In winter, the local RT increments were higher than in summer in BCN (ES) and SCH (NL) by factors of 2 and 4, respectively. Conversely, similar winter and summer local RT increments were observed in ZUE (CH), LMI (DE) and LEN (FR). For DE, van Pinxteren et al. (2016) have shown that for coarse particles urban background and traffic increments were broadly similar in year-round averages. It is important to note that the detection of a clear RT source at regional level in the selected countries and, consequently, the possibility to detect a regional RT increment, even if low, was due to the application of the multi-site PMF.

- ***Sources identified only at a subset of paired sites***

Biomass burning (anthropogenic)

On annual base the R+C BB increments were rather similar in CH (1.8 μg/m^3; 78% of *BB* contribution in ZUE), DE (1.1 μg/m^3; 77% of *BB* contribution in LMI/TRO) and in FR (1.1 μg/m^3; 42% of *BB* contribution in LEN). Notable difference was the relatively higher urban BB increment observed in LEN (1.5 μg/m^3; 58%) compared to LMI/TRO (0.3 μg/m^3; 23%) and ZUE (0.6 μg/m^3; 22%). Both the urban and R+C BB increments were much higher in winter compared to summer at the three paired sites where the BB source was detected. In CH, the R+C BB increment in winter reached around 3.9 μg/m^3 (73% of winter *BB* contribution in ZUE), whereas it was around 1.7-1.9 μg/m^3 in DE and FR. In winter, the highest urban increment was observed in LEN (FR; 2.7 μg/m^3; 59%).

Residual oil combustion (V-Ni) and Industrial (anthropogenic)

In both ES and NL (cf. Figures 6, S13 and S14 and Tables S7, S8 and S9), the local V-Ni increments were higher compared to the R+C V-Ni increments likely because of the influence of emissions from the port of Barcelona and Schiedam. Both the urban and R+C V-Ni increments were much higher in ES (1.7 μg/m^3 urban and 1.0 μg/m^3 R+C) than in NL (0.2 μg/m^3 urban and 0.1 μg/m^3 R+C), especially in summer when the urban and R+C increments in ES reached around 1.9 μg/m^3 (56%) and 1.5 μg/m^3 (44%), respectively. Thus, the V-Ni and the SSA local/R+C increments strongly contributed to the observed seasonal profile of PM measured in Barcelona.

On annual average, the urban and R+C IND increments were almost negligible in ES (0.04 μg/m^3 and 0.01 μg/m^3, respectively) compared to NL (0.3 μg/m^3 and 2.0

https://doi.org/10.5194/acp-2019-493
Preprint. Discussion started: 18 June 2019
© Author(s) 2019. CC BY 4.0 License.

Atmospheric Chemistry and Physics Discussions

μg/m^3, respectively). The R+C IND increments in NL were higher in summer (2.3 μg/m^3; 96%) compared to winter (1.7 μg/m^3; 95%). Mooibroek et al. (2011) showed that the IND source profile had slightly higher contributions during summer compared to the other seasons. Due to the lack of a pronounced seasonal pattern and the similar contribution at all Dutch receptor sites, Mooibroek et al. (2011) assumed the IND source was a common source representing negligible local contributions.

- ***Sources identified only at one paired site***

As already shown, two additional natural sources were detected in FR; m*arine biogenic* and *land biogenic* sources. These sources can be considered as totally natural. Thus, Lenschow's approach was not applied.

In DE, six extra sources were detected and among these sources the f*ungal spores* source was considered as totally regional/natural. For the other five sources, the Lenschow approach was applied, and the results are shown in Figure 6 and Table S6. Among these five sources, the contributions from CC and PHO sources were the highest. Both sources showed strong seasonal characters and were mostly of R+C origin. The R+C CC increment was much higher in winter (3.9 μg/m^3; 90% of CC source contribution to LMI) compared to summer (0.01 μg/m^3; 33%), whereas the R+C PHO increment was slightly higher in summer (2.2 μg/m^3; 83%) compared to winter (1.9 μg/m^3; 97%). As reported in van Pinxteren et al. (2016), coal combustion was a significant source only during easterly air mass inflow in winter and showed very similar concentrations at all sites included in van Pinxteren et al. (2016), highlighting the importance of trans-boundary air pollution transport in the study area. This, together with increased regional concentrations of biomass combustion (e.g. Hovorka et al., 2015) and secondary material, emphasizes the importance of transboundary pollution transport for regional air quality in the area of Leipzig.

4. CONCLUSIONS

This investigation aimed at discriminating local and R+C contributions from different sources to the concentrations of PM measured in five European cities. To accomplish this objective, we selected five paired sites in Europe (traffic/urban and regional/continental) providing PM chemically speciated data and applied the PMF model (EPA PMF v5.0). The obtained PM source contributions were then used to estimate the urban and non-urban (regional+continental; R+C) PM and source contributions increments through the application of Lenschow's approach. Urban increments were computed by withdrawing the rural source contributions to the local

https://doi.org/10.5194/acp-2019-493
Preprint. Discussion started: 18 June 2019
© Author(s) 2019. CC BY 4.0 License.

Atmospheric Chemistry and Physics Discussions

(urban) source contributions. In turn, regional increments were computed by withdrawing remote contributions (when available, i.e. in ES) to the regional contributions. For those countries where a remote site was not available, we did not separate the regional contributions from the continental contributions and the sum of the two (R+C) was calculated.

The results presented here provided a robust and feasible source allocation and estimation of the R+C increments to urban pollution. With the approach presented (multi-site PMF + Lenschow's approach), we were able to allocate urban pollution to major primary sources by activity sector or to main secondary aerosol fractions thanks to the application of the Positive Matrix Factorization (PMF) model that gathers together species emitted from the same source. Regarding source allocation for secondary aerosols, it is important to note that the sources such as shipping, agricultural activities, road transport, power generation, industry and domestic sector are important contributors of gaseous precursors and consequently to secondary aerosols. However, these separated contributions cannot be easily identified using PMF that tends to group in the same source (e.g. NSA) secondary nitrates formed from different sources. However, the PMF allocation for secondary aerosols presented here is extremely useful for models that can simulate, for example, NSA particles starting from emissions from different sectors. Moreover, this approach turns out to be useful in air quality management to assess both the sources and the relevance of local and regional emissions.

We have shown that we can use paired sites to estimate the relative contributions of local and R+C sources of PM. Sources of primary PM such as traffic dominate at the local scale while secondary PM like sulfate is mostly R+C in origin. However, NSA has a local component because of its rapid formation rates and the availability of NH_3 in urban settings. Other potentially important local sources of PM are emissions from ships, ports and industry especially in cities with harbors. We have shown that the amount of primary SSA emitted by ships depends on the amount of sulfur content in residual oil burned, and that it was much higher in NL compared to ES during 2007-2008. We have also shown that the primary SSA emitted by ships in NL was much lower in 2013-2014 compared to 2007-2008 due to change of fuel used by ships in berth and, in general, to the shift from high-sulfur to low-sulfur content fuels. Finally, potentially important regional sources are biomass burning and coal combustion.

The last EMEP report on air pollution trends in the EMEP region (Colette et al., 2016), reported on the significant negative trends observed at 38% (for PM_{10}) and 55% (for $PM_{2.5}$) of the sites during the period 2002 - 2012, with a relative change over the

https://doi.org/10.5194/acp-2019-493
Preprint. Discussion started: 18 June 2019
© Author(s) 2019. CC BY 4.0 License.

Atmospheric Chemistry and Physics Discussions

decade of -29% ([-29,-19]) and - 31% ([-35,-25]) for PM_{10} and $PM_{2.5}$, respectively. The observed reductions were mostly driven by the decrease of SO_4^{2-}, NO_3^- and NH_4^+ particles because of the reduction of the concentrations of gaseous precursors such as SO_2, NO_2 and NH_3. SO_2 and sulfate particles showed the strongest decreasing trends with median relative changes over the period 2002 – 2012 of -48% [-53,-38] and -39% [-42,-27], respectively. These decreases were even stronger during the period 1990 – 2001 with median relative changes of -80% [-82,-72] and -52% [-56,-46], respectively. NO_2 and particulate nitrate, cumulated with gaseous nitric acid (NO_3^-+HNO_3), showed lower decreasing trends of -17% [-20,18] and -7.1% [-12,18], respectively, during 2002 – 2012, and -28% [-34,-19] and -24% [-39,-9.8], respectively, during 1990 – 2001. Particulate NH_4^+ cumulated with gaseous NH_3 (NH_3+NH_4^+) showed decreasing trend of -14% [-15,23] and -40% [-47,-19], during the period 2002 – 2012 and 1990 – 2001, respectively. Recently, Pandolfi et al. (2016) reported total reductions of around 50% for both PM_{10} and $PM_{2.5}$ in Barcelona (UB; NE ES) during the period 2004 – 2014 and around 8% and 21%, for PM_{10} and $PM_{2.5}$, respectively, at regional level in NE of Spain (RB Montseny station). The sources that mostly contributed to the observed PM reductions were secondary SO_4^{2-}, secondary NO_3^- and residual oil combustion. The contributions from these sources decreased exponentially over the decade, with the sharpest decrease observed for secondary SO_4^{2-} in Barcelona mostly, but not only, because of the ban of heavy oils and petroleum coke for power generation around Barcelona from 2007 and the EC Directive on Large Combustion Plants, which resulted in the application of flue gas desulfurization (FGD) systems in a number of large facilities spread regionally. The fact that the trend of the secondary SO_4^{2-} source contribution in NE Spain was exponential suggested the attainment of a lower limit, and indicated a limited scope for further reduction of SO_2 emissions in NE of Spain. In fact, it has been estimated that the maximum in EU will be a further 20% SO_2 reduction through measures in industry, residential and commercial heating, maritime shipping, and reduced agricultural waste burning (UNECE, 2016). Conversely, in eastern European countries the scope for reduction is much greater and around 60% (UNECE, 2016).

For the present work, we used data collected over variable periods depending on the country and covering the period 2007 – 2014. Based on the analysis presented here, an improvement of air quality in the 5 cities included in this study could be achieved by further reducing local (urban) emissions of PM, NO_x and NH_3 (from both traffic and non-traffic sources) but also of PM and SO_2 from maritime ships and ports. Moreover, improvements can be achieved by reducing non-urban emissions of NH_3

https://doi.org/10.5194/acp-2019-493
Preprint. Discussion started: 18 June 2019
© Author(s) 2019. CC BY 4.0 License.

(agriculture), SO_2 (regional maritime shipping) and PM and gaseous precursors from regional BB sources, power generation, coal combustion and industries.

The possibility to detect pollutant sources is related to the PM chemical speciation available. We have shown here that BB emissions can be important contributors to PM, however, a clear determination of its contribution depends on the availability of specific BB tracers such as levoglucosan, or other specific polysaccharides, together with K^+. For the determination of residual oil combustion sources such as ships, whose emissions are projected to increase significantly if mitigation measures are not put in place swiftly, the determination of specific tracers such as V and Ni is necessary. Emissions from coal combustion, which we have seen to be important in central Europe, can be traced by using PAHs, As and Se, as important tracers of this source.

Data availability

The chemically speciated PM data used in this study are available upon request from the corresponding authors.

Code availability

The PMF model version 5.0 used in this study is available at https://www.epa.gov/air-research/positive-matrix-factorization-model-environmental-data-analyses.

Author contribution

AC, OT and MP developed the idea behind this study. MP performed the analysis, created the figures and wrote the manuscript. DM and EvdS applied the multi-site PMF on Dutch database. DvP and HH applied the multi-site PMF on German database. MP, DM and PH provided the analysis on primary sulfate emissions from ships in Spain and The Netherlands. XQ, AA, OF, CH, EP, VR, SS, provided guidance. All authors read and approved the final paper.

ACKNOWLEDGMENTS:

Measurements at Spanish sites (Montseny, Montsec and Barcelona) were supported by the Spanish Ministry of Economy, Industry and Competitiveness and FEDER funds under the project HOUSE (CGL2016-78594-R), and by the Generalitat de Catalunya (AGAUR 2014 SGR33, AGAUR 2017 SGR41 and the DGQA). Marco Pandolfi is funded by a Ramón y Cajal Fellowship (RYC-2013-14036) awarded by the Spanish Ministry of Economy and Competitiveness. The authors thank Cristina Reche, Noemi Pérez, and Anna Ripoll (IDAEA-CSIC) for providing chemically speciated PM data for Barcelona, Montseny, and Montsec stations (Spain). Measurements at French sites

https://doi.org/10.5194/acp-2019-493
Preprint. Discussion started: 18 June 2019
© Author(s) 2019. CC BY 4.0 License.

(Lens, Revin) were notably funded by the French Ministry of Environment ("Bureau de l'Air du Ministère de l'Ecologie, du Développement durable, et de l'Energie") and included in the CARA air quality monitoring and research project coordinated by the French reference laboratory for air quality monitoring (LCSQA), with technical support provided by the air quality monitoring networks Atmo Hauts-de-France and Atmo Grand-Est. IMT Lille Douai acknowledges financial support from the CaPPA project, which is funded by the French National Research Agency (ANR) through the PIA (Programme d'Investissement d'Avenir) under contract ANR-11-LABX-0005-01, and the CLIMIBIO project, both financed by the Regional Council "Hauts-de-France" and the European Regional Development Fund (ERDF). For the measurements at the German sites, financial support from the Saxon State Office for Environment, Agriculture and Geology (LfULG) is acknowledged. Gathering of in-situ data supporting this analysis was organized through the EMEP Task Force on Measurement and Modelling. The authors wish to thank D. C. Carslaw and K. Ropkins for providing the Openair software used in this paper.

BIBLIOGRAPHY:

Alastuey, A., Querol, X., Aas, W., Lucarelli, F., Pérez, N., Moreno, T., Cavalli, F., Areskoug, H., Balan, V., Catrambone, M., Ceburnis, D., Cerro, J. C., Conil, S., Gevorgyan, L., Hueglin, C., Imre, K., Jaffrezo, J.-L., Leeson, S. R., Mihalopoulos, N., Mitosinkova, M., O'Dowd, C. D., Pey, J., Putaud, J.-P., Riffault, V., Ripoll, A., Sciare, J., Sellegri, K., Spindler, G., and Yttri, K. E.: Geochemistry of PM10 over Europe during the EMEP intensive measurement periods in summer 2012 and winter 2013, Atmos. Chem. Phys., 16, 6107-6129, https://doi.org/10.5194/acp-16-6107-2016, 2016.

Amann, M., Bertok, I., Borken-Kleefeld, J., Cofala, J., Heyes, C., Höglund-Isaksson, L., Klimont, Z., Nguyen, B., Posch, M., Rafaj, P., Sander, R., Schöpp, W., Wagner, F., Winiwarter, W. (2011) Cost-effective control of air quality and greenhouse gases in Europe: modeling and policy applications. Environmental Modelling and Software 26, 1489–1501. doi:10.1016/j.envsoft.2011.07.012.

Amato, F., Pandolfi, M., Escrig, A., Querol, X., Alastuey, A., Pey, J., Perez, N., and Hopke, P. K.: Quantifying road dust resuspension in urban environment by Multilinear Engine: A comparison with PMF2, Atmos. Environ., 43, 2770–2780, 2009.

Bessagnet, B., Pirovano, G., Mircea, M., Cuvelier, C., Aulinger, A., Calori, G., Ciarelli, G., Manders, A., Stern, R., Tsyro, S., García Vivanco, M., Thunis, P., Pay, M.-T.,

https://doi.org/10.5194/acp-2019-493
Preprint. Discussion started: 18 June 2019
© Author(s) 2019. CC BY 4.0 License.

Atmospheric Chemistry and Physics Discussions

1258 Colette, A., Couvidat, F., Meleux, F., Rouïl, L., Ung, A., Aksoyoglu, S., Baldasano, J.
1259 M., Bieser, J., Briganti, G., Cappelletti, A., D'Isidoro, M., Finardi, S., Kranenburg, R.,
1260 Silibello, C., Carnevale, C., Aas, W., Dupont, J.-C., Fagerli, H., Gonzalez, L., Menut, L.,
1261 Prévôt, A. S. H., Roberts, P., and White, L.: Presentation of the EURODELTA III
1262 intercomparison exercise – evaluation of the chemistry transport models' performance
1263 on criteria pollutants and joint analysis with meteorology, Atmos. Chem. Phys., 16,
1264 12667–12701, https://doi.org/10.5194/acp-16-12667-2016, 2016.
1265
1266 Belis C. A., Pernigotti D., Pirovano G., Favez O., Jaffrezo J.L., Kuenen J., Denier van
1267 Der Gon H., Reizer M., Pay M.T., Almeida M., Amato F., Aniko A., Argyropoulos G.,
1268 Bande S., Beslic I., Bove M., Brotto P., Calori G., Cesari D., Colombi C., Contini D., De
1269 Gennaro G., Di Gilio A., Diapouli E., El Haddad I., Elbern H., Eleftheriadis K., Ferreira
1270 J., Foret G., Garcia Vivanco M., Gilardoni S., Hellebust S., Hoogerbrugge R.,
1271 Izadmanesh Y., Jorquera H., Karppinen A., Kertesz Z., Kolesa T., Krajsek K.,
1272 Kranenburg R., Lazzeri P., Lenartz F., Liora N., Long Y., Lucarelli F., Maciejewska K.,
1273 Manders A., Manousakas M., Martins H., Mircea M., Mooibroek D., Nava S., Oliveira
1274 D., Paatero P., Paciorek M., Paglione M., Perrone M., Petralia E., Pietrodangelo A.,
1275 Pillon S., Pokorna P., Poupkou A., Pradelle F., Prati P., Riffault V., Salameh D.,
1276 Samara C., Samek L., Saraga D., Sauvage S., Scotto F., Sega K., Siour G., Tauler R.,
1277 Valli G., Vecchi R., Venturini E., Vestenius M., Yarwood G., Yubero E., 2018 Results of
1278 the first European Source Apportionment intercomparison for Receptor and Chemical
1279 Transport Models, EUR 29254 EN, Publications Office of the European Union,
1280 Luxembourg, 2018, ISBN 978-92-79-86573-2, doi: 10.2760/41815, JRC 111887.
1281
1282 Brown, S.G., Eberly, S., Paatero, P., Norris, G.A.: Methods for estimating uncertainty in
1283 PMF solutions: Examples with ambient air and water quality data and guidance on
1284 reporting PMF results, Sci. of Tot. Environ., 518–519, 626-635,
1285 https://doi.org/10.1016/j.scitotenv.2015.01.022, 2015.
1286
1287 Bukowiecki, N., Lienemann, P., Hill, M., Furger, M., Richard, A., Amato, F., Prévôt,
1288 A.S.H., Baltensperger, U., Buchmann, B., Gehrig, R.: PM10 emission factors for non-
1289 exhaust particles generated by road traffic in an urban street canyon and along a
1290 freeway in Switzerland, Atm. Env., 44, 2330-2340, 2010.
1291
1292 Carslaw, D. C.: The openair manual – open-source tools for analysing air pollution
1293 data, Manual for version 0.7-0, King's College, London, 2012.
1294

https://doi.org/10.5194/acp-2019-493
Preprint. Discussion started: 18 June 2019
© Author(s) 2019. CC BY 4.0 License.

1295 Carslaw, D. C. and Ropkins, K.: openair – an R package for air quality data analysis,
1296 Environ. Modell. Softw., 27–28, 52–61, 2012.
1297
1298 Colette, A., Aas, W., Banin, L., Braban, C.F., Ferm, M., González Ortiz, A., Ilyin, I.,
1299 Mar, K., Pandolfi, M., Putaud, J.-P., Shatalov, V., Solberg, S., Spindler, G., Tarasova,
1300 O., Vana, M., Adani, M., Almodovar, P., Berton, E., Bessagnet, B., Bohlin-Nizzetto, P.,
1301 Boruvkova, J., Breivik, K., Briganti, G., Cappelletti, A., Cuvelier, K., Derwent, R.,
1302 D'Isidoro, M., Fagerli, H., Funk, C., Garcia Vivanco, M., González Ortiz, A., Haeuber,
1303 R., Hueglin, C., Jenkins, S., Kerr, J., de Leeuw, F., Lynch, J., Manders, A., Mircea, M.,
1304 Pay, M.T., Pritula, D., Putaud, J.-P., Querol, X., Raffort,V., Reiss, I., Roustan, Y.,
1305 Sauvage, S., Scavo, K., Simpson, D., Smith, R.I., Tang, Y.S., Theobald, M., Tørseth,
1306 K., Tsyro, S., van Pul, A., Vidic, S., Wallasch, M., Wind, P., Air pollution trends in the
1307 EMEP region between 1990 and 2012, Joint Report of the EMEP Task Force on
1308 Measurements and Modelling (TFMM), Chemical Co-ordinating Centre (CCC),
1309 Meteorological Synthesizing Centre-East (MSC-E), Meteorological Synthesizing
1310 Centre-West (MSC-W), EMEP/CCC-Report 1/2016.
1311
1312 Escrig, A., Monfort, E., Celades, I., Querol, X., Amato, F., Minguillon, M. C., and
1313 Hopke, P. K.: Application of optimally scaled target factor analysis for assessing source
1314 contribution of ambient PM10, J. Air Waste Manage., 59, 1296–1307, 2009.
1315 Lenschow, P., Abraham, H.-J., Kutzner, K., Lutz, M., Preu, J.-D., Reichenbacher, W.:
1316 Some ideas about the sources of PM10, Atm. Env., 35, 1, S23–S33, 2001.
1317 EEA: European Environment Agency, Air quality in Europe, Report No 12/2018, ISSN
1318 1977-8449, doi: 10.2800/777411, 2018.
1319
1320 Gehrig, R., and Buchmann, B.: Characterising seasonal variations and spatial
1321 distribution of ambient PM10 and PM2.5 concentrations based on long-term Swiss
1322 monitoring data, Atm. Env., 37(19), 2571-2580, https://doi.org/10.1016/S1352-
1323 2310(03)00221-8, 2003.
1324
1325 Gianini, M.F.D., Fischer, A., Gehrig, R., Ulrich, A., Wichser, A., Piot, C., Besombes, J.-
1326 L., Hueglin, C.: Comparative source apportionment of PM10 in Switzerland for
1327 2008/2009 and 1998/1999 by Positive Matrix Factorisation, Atm. Env., 54, 149-158,
1328 2012.
1329

https://doi.org/10.5194/acp-2019-493
Preprint. Discussion started: 18 June 2019
© Author(s) 2019. CC BY 4.0 License.

1330 Godoy, M., Godoy, J.M., Artaxo, P.: Aerosol source apportionment around a large coal
1331 fired power plant e thermoelectric complex Jorge Lacerda, Santa Catarina, Brazil. Atm.
1332 Env., 39, 5307-5324, 2005.
1333
1334 Hopke, P.K.: Review of receptor modeling methods for source apportionment, Journal
1335 of the Air & Waste Management Association, 66:3, 237-259, DOI:
1336 10.1080/10962247.2016.1140693.
1337
1338 Hovorka, J., Pokorná, P., Hopke, P.K., Křůmal, K., Mikuška, P., Píšová, M.: Wood
1339 combustion, a dominant source of winter aerosol in residential district in proximity to a
1340 large automobile factory in Central Europe, J., Atm. Environ., 113, 98- 107, 2015.
1341
1342 Hueglin, C., Gehrig, R., Baltensperger, U., Gysel, M., Monn, C., Vonmont, H.: Chemical
1343 characterisation of PM2.5, PM10 and coarse particles at urban, near city and rural sites
1344 in Switzerland, Atm. Env., 39, 637-651, 2005.
1345
1346 IPCC, 2013: Climate Change 2013: The Physical Science Basis. Contribution of
1347 Working Group I to the Fifth Assessment Report of the Intergovernmental Panel on
1348 Climate Change [Stocker, T.F., D. Qin, G.-K. Plattner, M. Tignor, S.K. Allen, J.
1349 Boschung, A. Nauels, Y. Xia, V. Bex and P.M. Midgley (eds.)]. Cambridge University
1350 Press, Cambridge, United Kingdom and New York, NY, USA, 1535, 2013..
1351
1352 Kiesewetter, G., Borken-Kleefeld, J., Schöpp, W., Heyes, C., Thunis, P., Bessagnet, B.,
1353 Terrenoire, E., Fagerli, H., Nyiri, A., and Amann, M.: Modelling street level PM10
1354 concentrations across Europe: source apportionment and possible futures, Atmos.
1355 Chem. Phys., 15, 1539-1553, https://doi.org/10.5194/acp-15-1539-2015, 2015.
1356
1357 Kim E., Hopke P.K., Edgerton E.S.: Source identification of Atlanta aerosol by positive
1358 matrix factorization Journal of the Air and Waste Management Association, 53, 731-
1359 739, 2003.
1360
1361 Kim, E., Hopke, P.K.: Source characterization of ambient fine particles at multiple sites
1362 in the Seattle area, Atm. Env., 42, 6047–6056, 2008.
1363
1364 Kranenburg, R., Segers, A.J., Hendriks, C., Schaap, M.: Source apportionment using
1365 LOTOS-EUROS: Module description and evaluation, Geosci. Model Dev., 6, 721-733,
1366 2013.

https://doi.org/10.5194/acp-2019-493
Preprint. Discussion started: 18 June 2019
© Author(s) 2019. CC BY 4.0 License.

Lanz, V. A., Alfarra, M. R., Baltensperger, U., Buchmann, B., Hueglin, C., Szidat, S., Wehrli, M. N., Wacker, L., Weimer, S., Caseiro, A., Puxbaum, H., and Prevot, A. S. H.: Source attribution of submicron organic aerosols during wintertime inversions by advanced factor analysis of aerosol mass spectra, Environ. Sci. Technol., 42, 214–220, 2008.

Lenschow, P., Abraham, H.-J., Kutzner, K., Lutz, M., Preu, J.-D., Reichenbacher, W.: Some ideas about the sources of PM10, Atmos. Environ., 35, 23–33, 2001.

Millán, M. M., Salvador, R., Mantilla, E., Kallos, G.: Photo-oxidant dynamics in the Mediterranean Basin in Summer: Results from European Research Projects. J. Geophys. Res., 102, D7, 8811-8823, 1997.

Millán, M. M., E. Mantilla, R. Salvador, A. Carratalá, Mª.J. Sanz, L. Alonso, G. Gangoiti, M. Navazo, 2000: Ozone cycles in the Western Mediterranean Basin: Interpretation of Monitoring Data in Complex Coastal Terrain. J. Appl. Meteor., 39, 487-508.

Mohr, C., DeCarlo, P. F., Heringa, M. F., Chirico, R., Slowik, J. G., Richter, R., Reche, C., Alastuey, A., Querol, X., Seco, R., Peñuelas, J., Jiménez, J. L., Crippa, M., Zimmermann, R., Baltensperger, U., and Prévôt, A. S. H.: Identification and quantification of organic aerosol from cooking and other sources in Barcelona using aerosol mass spectrometer data, Atmos. Chem. Phys., 12, 1649-1665, https://doi.org/10.5194/acp-12-1649-2012, 2012.

Mooibroek, D., Schaap, M., Weijers, E.P., Hoogerbrugge, R.: Source apportionment and spatial variability of PM2.5 using measurements at five sites in the Netherlands, Atm. Env., 45, 4180-4191, 2011.

Mooibroek, D., Staelens, J., Cordell, R., Panteliadis, P., Delaunay, T., Weijers, E., Vercauteren, J., Hoogerbrugge, R., Dijkema, M., Monks, P.A., Roekens, E.: PM10 source apportionment in Five North Western European Cities – Outcome of the Joaquin Project, in Issues in Environmental Science and Technology No 42, Airborne Particulate Matter: Sources, Atmospheric Processes and Health, Edited by R.E. Hester, R.M. Harrison and X. Querol, The Royal Society of Chemistry, ISNN 1350-7583, 2016.

https://doi.org/10.5194/acp-2019-493
Preprint. Discussion started: 18 June 2019
© Author(s) 2019. CC BY 4.0 License.

1403 Paatero, P. and Tapper, U.: Positive matrix factorization: A nonnegative factor model
1404 with optimal utilization of error estimates of data values, Environmetrics, 5, 111–126,
1405 1994.
1406
1407 Paatero, P.: Least squares formulation of robust non-negative factor analysis.
1408 Chemometrics and Intelligent Laboratory Systems, 37, 23–35, 1997.
1409
1410 Paatero, P.: The multilinear engine – a table-driven least squares program for solving
1411 multilinear problems, including the n-way parallel factor analysis model, J. Comput.
1412 Graph. Stat., 8, 854–888, 1999.
1413
1414 Paatero, P., Hopke, P. K., Song, X., and Ramadan, Z.: Understanding and controlling
1415 rotations in factor analytic models, Chemometr. Intell. Lab., 60, 253–264, 2002.
1416
1417 Paatero, P. and Hopke, P. K.: Discarding or downweighting high noise variables in
1418 factor analytic models, Anal. Chim. Acta, 490, 277–289, 2003.
1419
1420 Paatero, P.: User's guide for positive matrix factorization programs PMF2 and PMF3,
1421 Part 1: tutorial, University of Helsinki, Helsinki, Finland, 2004.
1422
1423 Paatero, P. and Hopke, P. K.: Rotational tools for factor analytic models implemented
1424 by using the multilinear engine, Chemometrics, 23, 91–100, 2008.
1425
1426 Paatero, P., Eberly, S., Brown, S.G., Norris, G.A., Methods for estimating uncertainty in
1427 factor analytic solutions. Atmos. Meas. Tech. 7, 781–797, 2014.
1428 Pandolfi, M., Cusack, M., Alastuey, A., and Querol, X.: Variability of aerosol optical
1429 properties in the Western Mediterranean Basin, Atmos. Chem. Phys., 11, 8189–8203,
1430 https://doi.org/10.5194/acp-11-8189-2011, 2011.
1431
1432 Pandolfi, M., Gonzalez-Castanedo, Y., Alastuey, A., de la Rosa, J., Mantilla, E.,
1433 Sanchez de la Campa, A., Querol, X., Pey, J., Amato, F., Moreno, T.: Source
1434 apportionment of PM10 and PM2.5 at multiple sites in the strait of Gibraltar by PMF:
1435 impact of shipping emissions, Environ. Sci. Pollut. Res., 18, 260–269, 10.1007/s11356-
1436 010-0373-4, 2011a.
1437

https://doi.org/10.5194/acp-2019-493
Preprint. Discussion started: 18 June 2019
© Author(s) 2019. CC BY 4.0 License.

1438 Pandolfi, M., Amato, F., Reche, C., Alastuey, A., Otjes, R. P., Blom, M. J., and Querol,
1439 X.: Summer ammonia measurements in a densely populated Mediterranean city,
1440 Atmos. Chem. Phys., 12, 7557-7575, https://doi.org/10.5194/acp-12-7557-2012, 2012.
1441
1442 Pandolfi, M., et al.: Effects of sources and meteorology on particulate matter in the
1443 Western Mediterranean Basin: An overview of the DAURE campaign, J. Geophys. Res.
1444 Atmos., 119, 4978–5010, doi:10.1002/2013JD021079, 2014.
1445
1446 Pandolfi, M., Ripoll, A., Querol, X., and Alastuey, A.: Climatology of aerosol optical
1447 properties and black carbon mass absorption cross section at a remote high-altitude
1448 site in the western Mediterranean Basin, Atmos. Chem. Phys., 14, 6443-6460,
1449 https://doi.org/10.5194/acp-14-6443-2014, 2014a.
1450
1451 Pandolfi, M., Alastuey, A., Pérez, N., Reche, C., Castro, I., Shatalov, V., and Querol,
1452 X.: Trends analysis of PM source contributions and chemical tracers in NE Spain
1453 during 2004–2014: a multi-exponential approach, Atmos. Chem. Phys., 16, 11787-
1454 11805, https://doi.org/10.5194/acp-16-11787-2016, 2016.
1455
1456 Pérez, N., Pey, J., Castillo, S., Viana, M., Alastuey, A., and Querol, X.: Interpretation of
1457 the variability of levels of regional background aerosols in the Western Mediterranean,
1458 Sci. Total Environ., 407, 527–540, 2008.
1459
1460 Pey, J., Pérez, N., Querol, X., Alastuey, A., Cusack, M., and Reche, C.: Intense winter
1461 atmospheric pollution episodes affecting the Western Mediterranean, Sci. Total
1462 Environ., 408, 1951–1959, 2010.
1463
1464 Pey, J., Querol, X., Alastuey, A., Forastiere, F., and Stafoggia, M.: African dust
1465 outbreaks over the Mediterranean Basin during 2001–2011: PM10 concentrations,
1466 phenomenology and trends, and its relation with synoptic and mesoscale meteorology,
1467 Atmos. Chem. Phys., 13, 1395-1410, https://doi.org/10.5194/acp-13-1395-2013, 2013.
1468
1469 Pisoni, E., Clappier, A., Degraeuwe, B., Thunis, P.: Adding spatial flexibility to source-
1470 receptor relationships for air quality modeling, Environ.l Mod. & Soft., 90, 68-77,
1471 https://doi.org/10.1016/j.envsoft.2017.01.001, 2017.
1472

https://doi.org/10.5194/acp-2019-493
Preprint. Discussion started: 18 June 2019
© Author(s) 2019. CC BY 4.0 License.

1473 Polissar, A. V., Hopke, P. K., Paatero, P., Malm, W. C., and Sisler, J. F.: Atmospheric
1474 aerosol over Alaska 2. Elemental composition and sources, J. Geophys. Res.-Atmos.,
1475 103, 19045–19057, 1998.
1476
1477 Pokorná, P., Hovorka, J., Hopke, P.K., Kroužek, J.: PM1-10 source apportionment in a
1478 village situated in industrial region of Central Europe, J. Air Waste Manage. Assoc., 63,
1479 1412-1421, 2013.
1480
1481 Pokorná, P., Hovorka, J., Klán, M., Hopke, P.K.: Source apportionment of size resolved
1482 particulate matter at a European air pollution hot spot, , Sci. of the Tot. Environ., 502,
1483 172–183, 2015.
1484
1485 Querol, X., Viana, M., Alastuey, A., Amato, F., Moreno, T., Castillo, S., Pey, J., de la
1486 Rosa, J., Artíñano, B., Salvador, P., García Dos Santos, S., Fernández-Patier, R.,
1487 Moreno-Grau, S., Negral, L., Minguillón, M. C., Monfort, E., Gil, J. I., Inza, A., Ortega,
1488 L. A., Santamaría, J. M., and Zabalza, J.: Source origin of trace elements in PM from
1489 regional background, urban and industrial sites of Spain, Atmos. Environ., 41, 7219–
1490 7231, 2007.
1491
1492 Querol, X., Alastuey, A., Lopez-Soler, A., Plana, F; Puicercus, J.A., Mantilla, E., Palau,
1493 J.L.: Daily evolution of sulphate aerosols in a rural area, northeastern Spain-elucidation
1494 of an atmospheric reservoir effect, Environ. Poll., 105, 397-407, 1999.
1495
1496 Querol, X., Viana, M., Alastuey, A., Amato, F., Moreno, T., Castillo, S., Pey, J., de la
1497 Rosa, J., Artíñano, B., Salvador, P., García Dos Santos, S., Fernández-Patier, R.,
1498 Moreno-Grau, S., Negral, L., Minguillón, M. C., Monfort, E., Gil, J. I., Inza, A., Ortega,
1499 L. A., Santamaría, J. M., and Zabalza, J.: Source origin of trace elements in PM from
1500 regional background, urban and industrial sites of Spain, Atmos. Environ., 41, 7219–
1501 7231, 2007.
1502
1503 Querol, X., Alastuey, A., Moreno, T., Viana, M.M., Castillo, S., Pey, J., Rodríguez, S.,
1504 Artiñano, B., Salvador, P., Sánchez, M., Garcia Dos Santos, S., Herce Garraleta, M.
1505 D., Fernandez-Patier, R., Moreno-Grau, S., Negral, L., Minguillón, M. C., Monfort, E.,
1506 Sanz, M. J., Palomo-Marín, R., Pinilla-Gil, E., Cuevas, E., de la Rosa, J., and Sánchez
1507 de la Campa, A.: Spatial and temporal variations inairborne particulate matter (PM10
1508 and PM2.5) across Spain 1999–2005, Atmos. Environ., 42, 3694–3979, 2008.
1509

https://doi.org/10.5194/acp-2019-493
Preprint. Discussion started: 18 June 2019
© Author(s) 2019. CC BY 4.0 License.

1510 Querol, X., Pey, J., Pandolfi, M., Alastuey, A., Cusack, M., Pérez, N., Moreno, T.,Viana,
1511 M., Mihalopoulos, N., Kallos, G., Kleanthous, S.: African dust contributions to mean
1512 ambient PM10 mass-levels across the Mediterranean Basin, Atm. Env., 43, 4266–
1513 4277, 2009.
1514
1515 Reche, C., Viana, M., Pandolfi, M., Alastuey, A., Moreno, T., Amato, F., Ripoll, A., and
1516 Querol, X.: Urban NH3 levels and sources in a Mediterranean environment, Atmos.
1517 Environ., 57, 153–164, 2012
1518
1519 Ripoll, A., Pey, J., Minguillón, M. C., Pérez, N., Pandolfi, M., Querol, X., and Alastuey,
1520 A.: Three years of aerosol mass, black carbon and particle number concentrations at
1521 Montsec (southern Pyrenees, 1570 m a.s.l.), Atmos. Chem. Phys., 14, 4279-4295,
1522 https://doi.org/10.5194/acp-14-4279-2014, 2014.
1523
1524 Sanz, M. J., Palomo-Marín, R., Pinilla-Gil, E., Cuevas, E., de la Rosa, J., and Sánchez
1525 de la Campa, A.: Spatial and temporal variations inairborne particulate matter (PM10
1526 and PM2.5) across Spain 1999–2005, Atmos. Environ., 42, 3694–3979, 2008.
1527
1528 Seibert P., Kromp-Kolb H., Baltensperger U., Jost D.T., Schwikowski M.: Trajectory
1529 Analysis of High-Alpine Air Pollution Data, in: Gryning SE., Millán M.M. (eds) Air
1530 Pollution Modeling and Its Application X. NATO · Challenges of Modern Society, vol 18.
1531 Springer, Boston, MA, 1994.
1532
1533 Sofowote, U. M., Su, Y., Dabek-Zlotorzynska, E., Rastogi, A. K., Brook, J., and Hopke,
1534 P. K.: Sources and temporal variations of constrained PMF factors obtained from
1535 multiple-year receptor modeling of ambient PM2.5 data from five speciation sites in
1536 Ontario, Canada, Atmos. Environ., 108, 140–150, 2015.
1537
1538 Stelson, A.W. and Seinfeld, J.H.: Relative humidity and temperature dependence of the
1539 ammonium nitrate dissociation constant, Atm. Env., 16, 983-992, 1967.
1540
1541 Szidat, S., Jenk, T.M., Synal, H.A., Kalberer, M., Wacker, L., Hajdas, I., Kasper-Giebl,
1542 A., Baltensperger, U.: Contributions of fossil fuel, biomass-burning, and biogenic
1543 emissions to carbonaceous aerosols in Zurich as traced by C-14, Journal of
1544 Geophysical Research-Atmospheres 111, 12, 2006.
1545

https://doi.org/10.5194/acp-2019-493
Preprint. Discussion started: 18 June 2019
© Author(s) 2019. CC BY 4.0 License.

1546 Thunis, P.: On the validity of the incremental approach to estimate the impact of cities
1547 on air quality, Atmos. Environ., 173, 210-222, 2018.
1548
1549 UNECE: Towards Cleaner Air. Scientific Assessment Report. EMEP Steering Body and
1550 Working Group on Effects of the Convention on Long-Range Transboundary Air
1551 Pollution, Oslo, 50 pp., edited by: Maas, R. and Grennfelt, P.,
1552 www.unece.org/environmental-policy/conventions/envlrtapwelcome/publications.html
1553 (last access: 16 April 2019), 2016.
1554
1555 van Pinxteren, D., Fomba, K. W., Spindler, G., Mueller, K., Poulain, L., Iinuma, Y.,
1556 Loschau, G., Hausmann A., and Herrmann, H.: Regional air quality in Leipzig,
1557 Germany: detailed source apportionment of size resolved aerosol particles and
1558 comparison with the year 2000, Faraday Discuss., 189, 291-315, 2016.
1559
1560 Van Damme, M., Clarisse, L., Whitburn, S., Hadji-Lazaro, J., Hurtmans, D., Clerbaux,
1561 C., Coheur, P.F.: Industrial and agricultural ammonia point sources exposed, Nature
1562 564, 99–103, 2018.
1563
1564 Waked, A., Favez, O., Alleman, L. Y., Piot, C., Petit, J.-E., Delaunay, T., Verlinden, E.,
1565 Golly, B., Besombes, J.-L., Jaffrezo, J.-L., and Leoz-Garziandia, E.: Source
1566 apportionment of PM10 in a north-western Europe regional urban background site
1567 (Lens, France) using positive matrix factorization and including primary biogenic
1568 emissions, Atmos. Chem. Phys., 14, 3325-3346, https://doi.org/10.5194/acp-14-3325-
1569 2014, 2014.
1570